



IXPE
Imaging
X-Ray
Polarimetry
Explorer

Рентгеновская поляриметрия со спутника IXPE

**Juri Poutanen
(University of Turku & IKI RAS)**

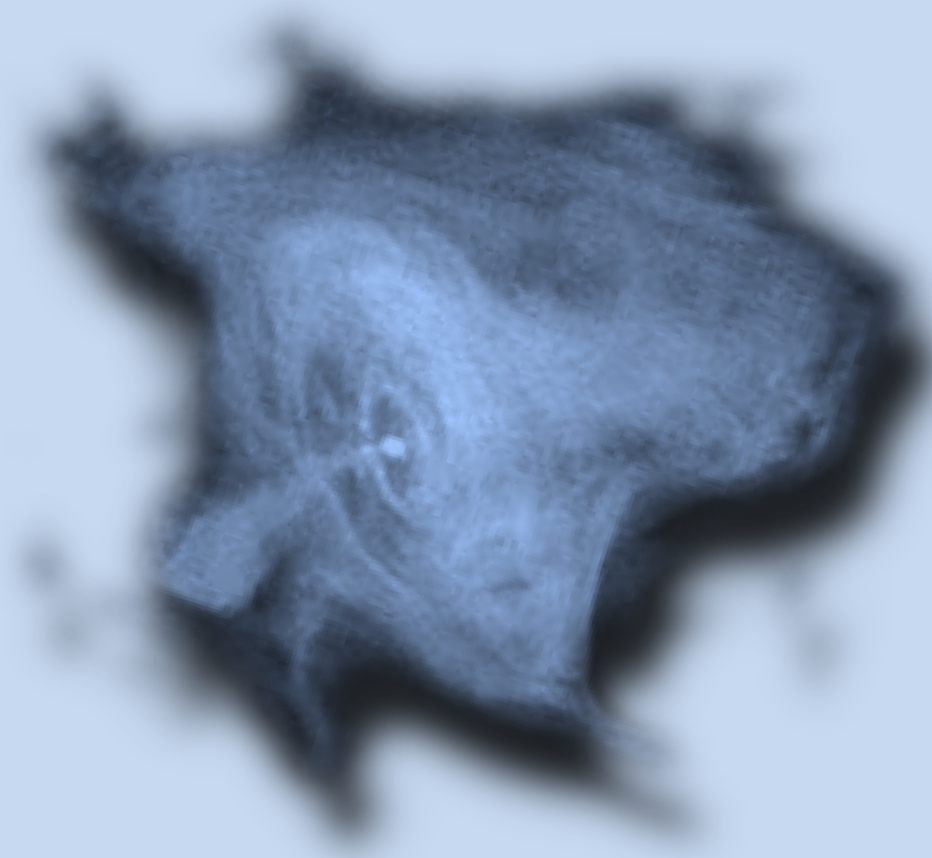
**2022 December 20
IKI RAS**



Introduction

Polarimetry has been proved very important in radio, IR and optical bands.

In X-rays, where non-thermal emission processes and aspherical geometries are common, linear polarimetry is crucial to understand emitting sources.

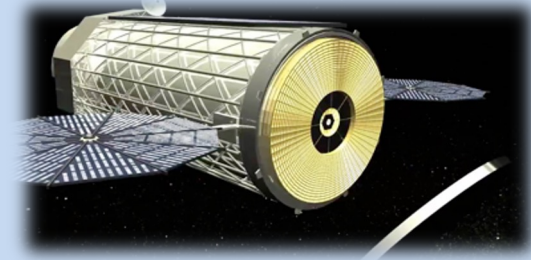


However, only one measurement ($P=19\%$ for the Crab Nebula, demonstrating synchrotron emission) has been obtained so far, back in the 70's.

Some history

- ✓ X-ray polarimeter planned in the original design of the *Einstein* observatory (1978) but removed by descoping the mission
 - ✓ X-ray polarimeter(s) planned for the original *SRG* mission (1993) but never launched
 - ✓ *GEMS* selected as a NASA SMEX mission but cancelled (2012)
 - ✓ X-ray Polarimeter planned to be on board on *XEUS*, then *IXO* – never flew
-
- Major obstacle: X-ray polarimetry requires more observing time than imaging, timing, and spectroscopy
 - X-ray polarimetry is risky! Only one (+1) object detected.
 - Dare to open a new frontier. Seize the unknown.

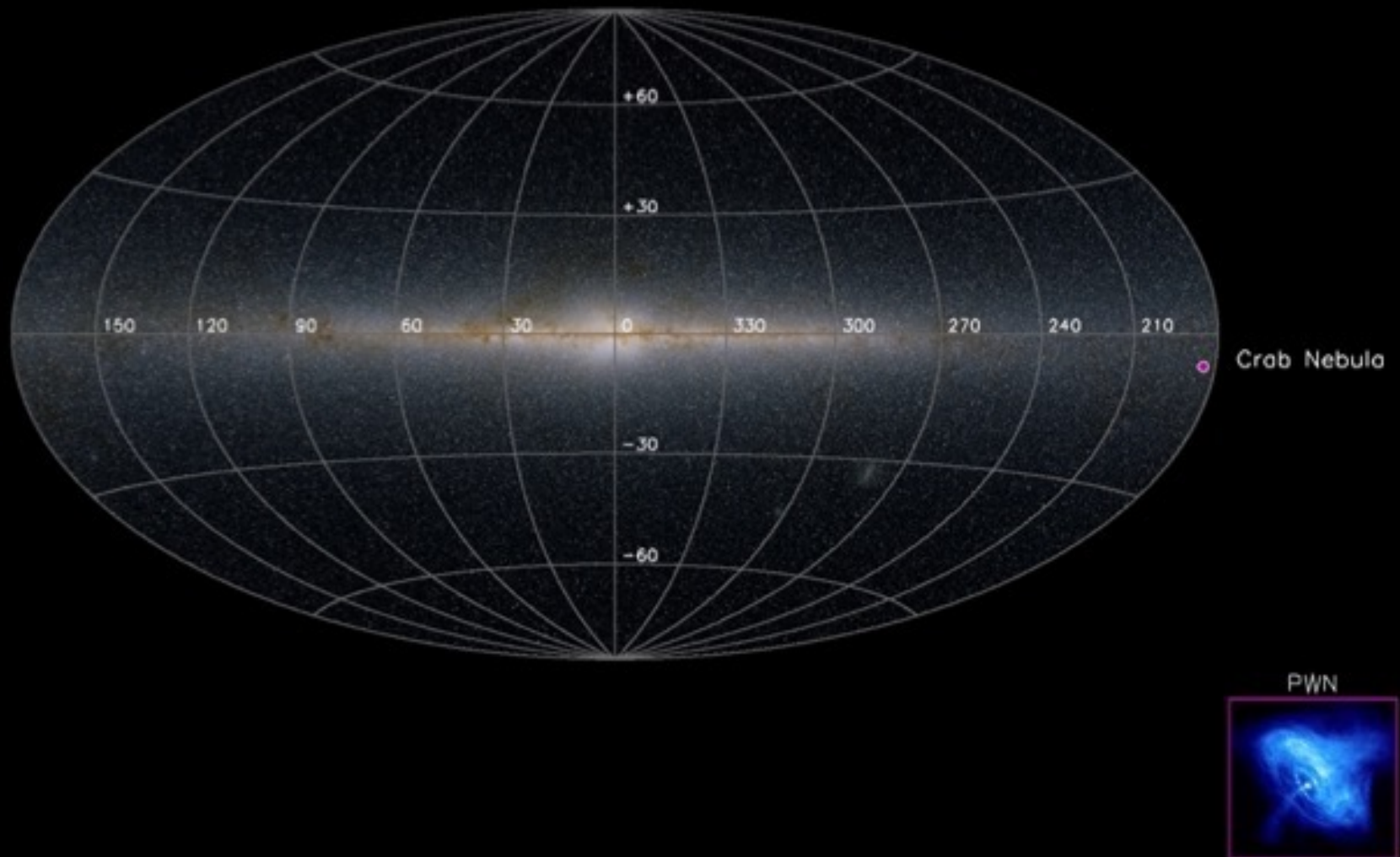
HEAO 2 OBSERVATORY





IXPE
Imaging
X-Ray
Polarimetry
Explorer

Map of polarized X-ray sources in 2021





IXPE
Imaging
X-Ray
Polarimetry
Explorer

IXPE launched on 2021 Dec 9



SpaceX Falcon 9



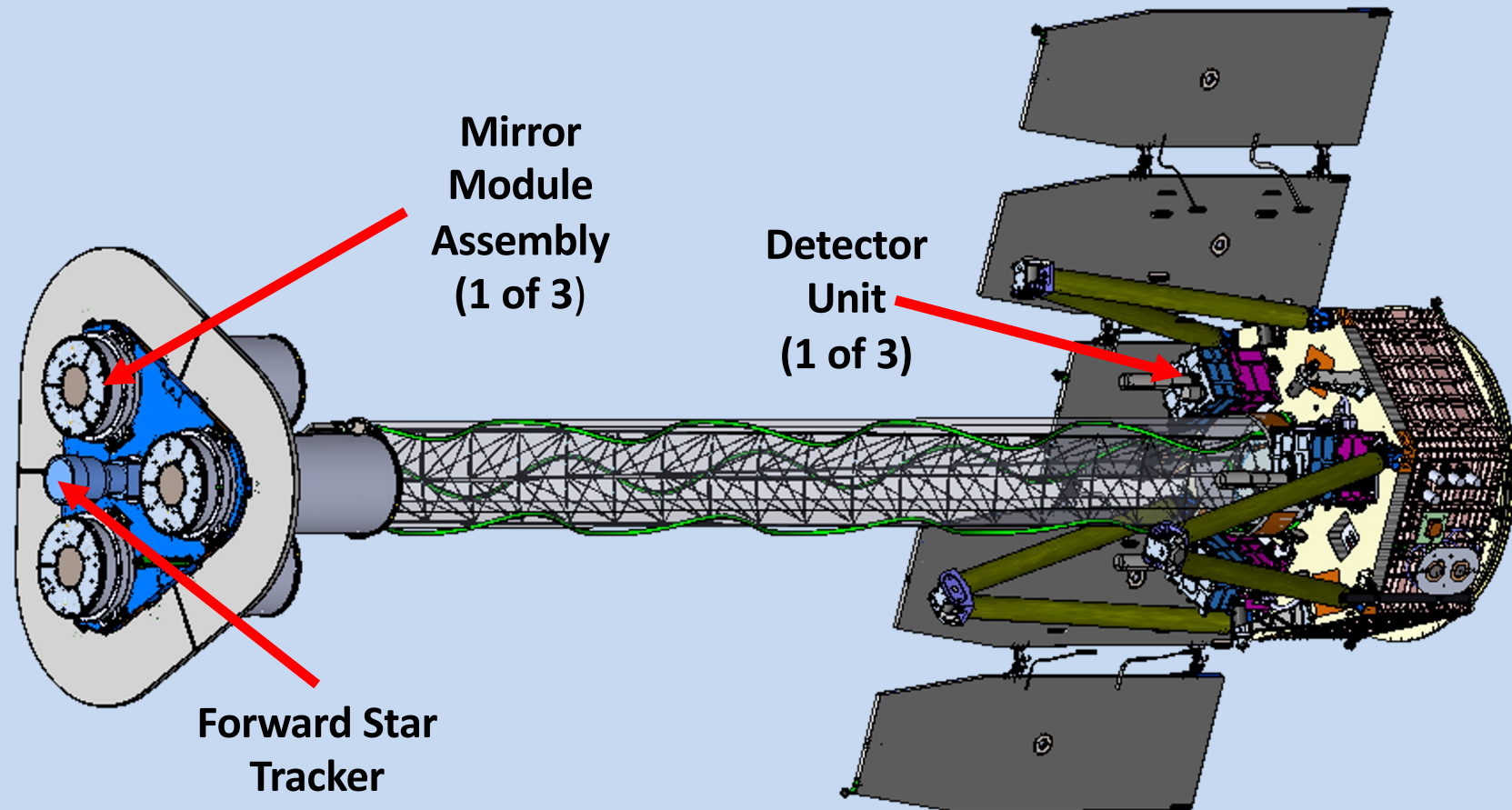
Jordan Sirokie

APOD ©Jordan Sirokie



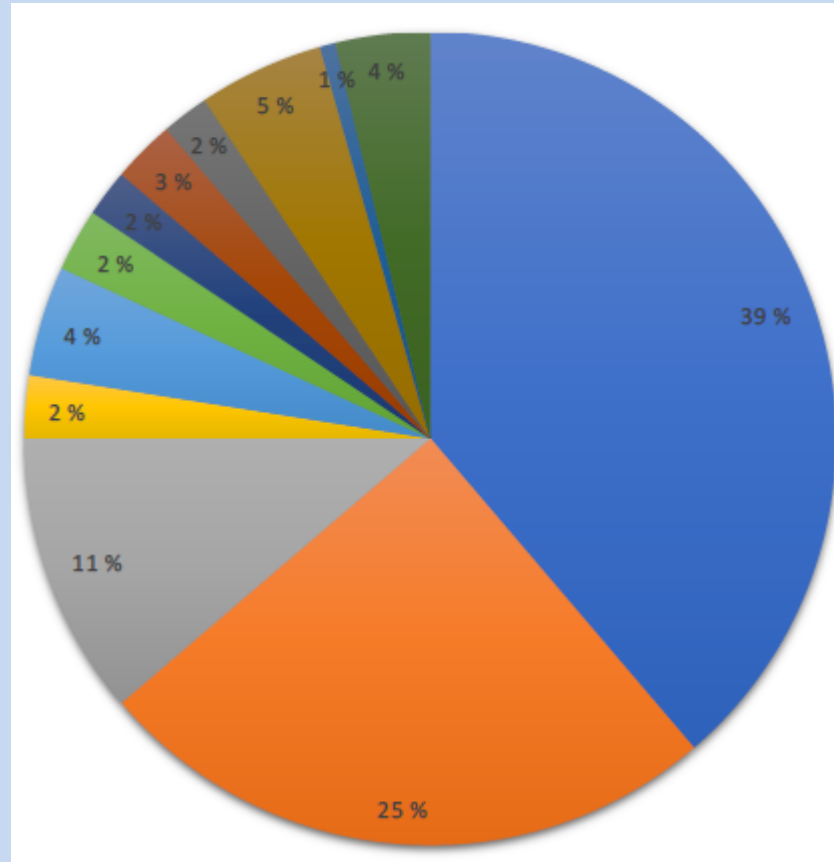
IXPE
Imaging
X-Ray
Polarimetry
Explorer

IXPE



5.2 m total length
4.0 m focal length

The IXPE Team



160 scientists from 12 countries



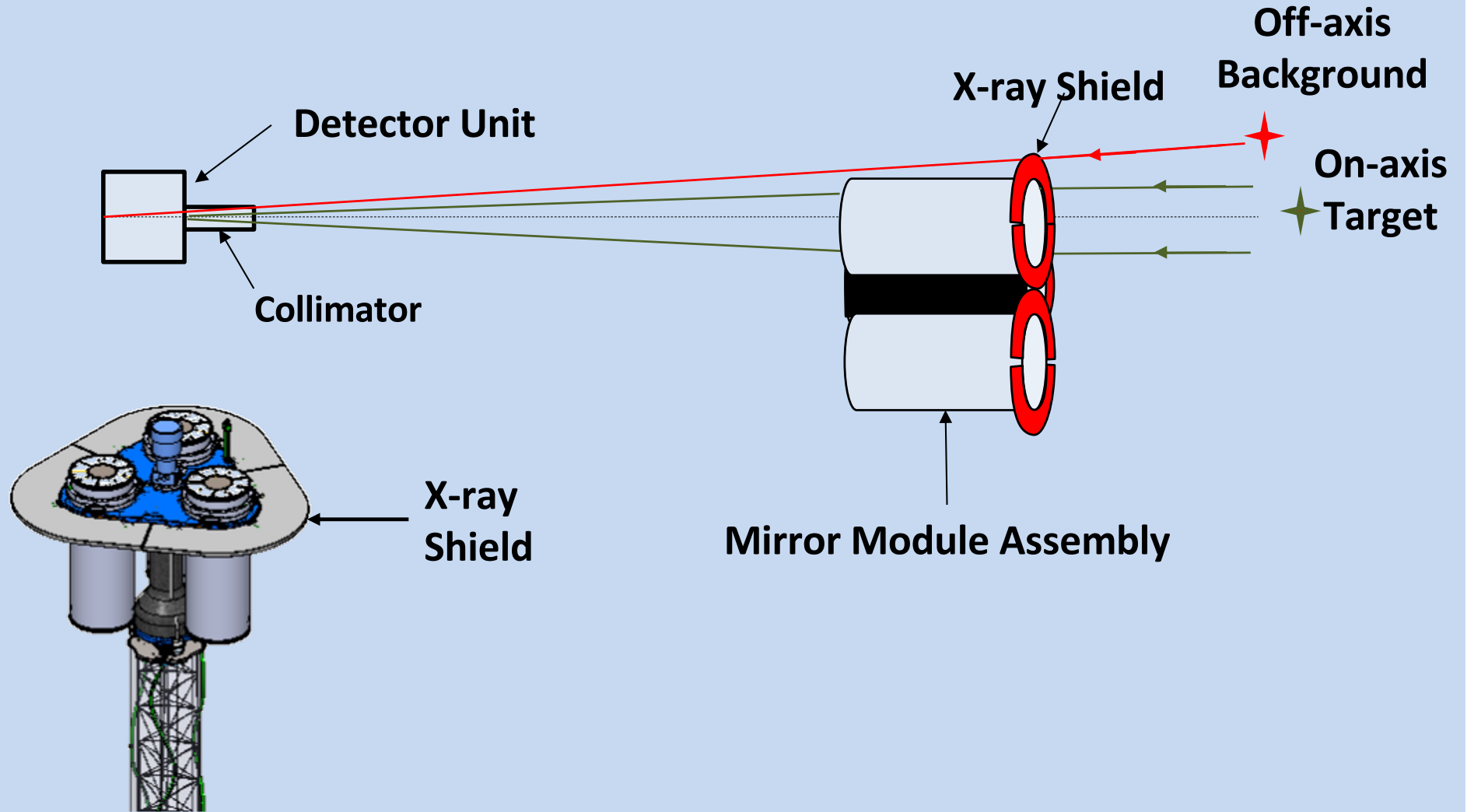
The Working Groups

- **PI: Steven O'Dell (from Dec 2022; Martin Weisskopf until May 2022 and then Brian Ramsey)**
- **Project scientist: Steven Ehlert (MSFC)**
- **Science Working Group (SWG)**
 - I. Donnarumma (IT) & S. Ehlert (US), Co-Chairs
- **Science Advisory Team (SAT)**
 - G. Matt (IT) & R. Romani (US), Co-Chairs
- **SAT Topical Working Groups (TWG), Leads**
 - Pulsar Wind Nebula & Radio Pulsars, N. Bucciantini (IT)
 - Supernova remnants, P. Slane (US)
 - Accreting stellar-mass black holes, M. Dovčiak (CZ)
 - Accreting neutron stars, J. Poutanen (FI)
 - Magnetars, R. Turolla (IT)
 - Radio-quiet AGN and Sgr A*, F. Marin (FR)
 - Blazars & radio galaxies, A. Marscher (US)
- **Calibration Working Group**
 - W. Baumgartner (US), F. Muleri (IT), & J. Kolodziejczak (US)
- **Science Analysis & Simulation Working Group**
 - L. Baldini (IT) & H. Marshall (US)



IXPE
Imaging
X-Ray
Polarimetry
Explorer

Shield and Collimator Suppress Background

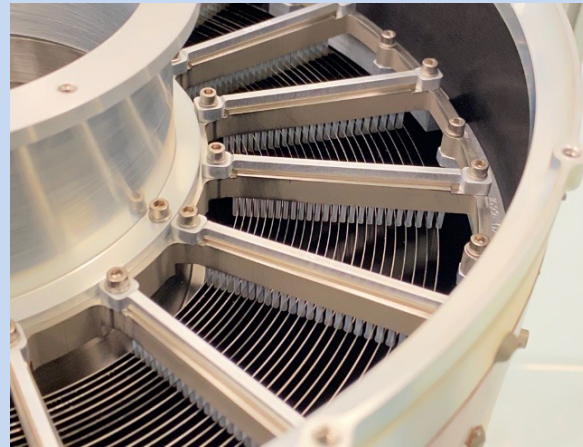


The Optics

Parameter	Value
Number of mirror modules	3
Number of shells per mirror module	24
Focal length	4 m
Total shell length	600 mm
Range of shell diameters	162–272 mm
Range of shell thicknesses	0.16–0.25 mm
Shell material	Electroformed nickel–cobalt alloy
Effective area per mirror module	166 cm ² (@ 2.3 keV); > 175 cm ² (3–6 keV)
Angular resolution (HPD)	≤ 27 arcsec
Field of view (detector limited)	12.9 arcmin square



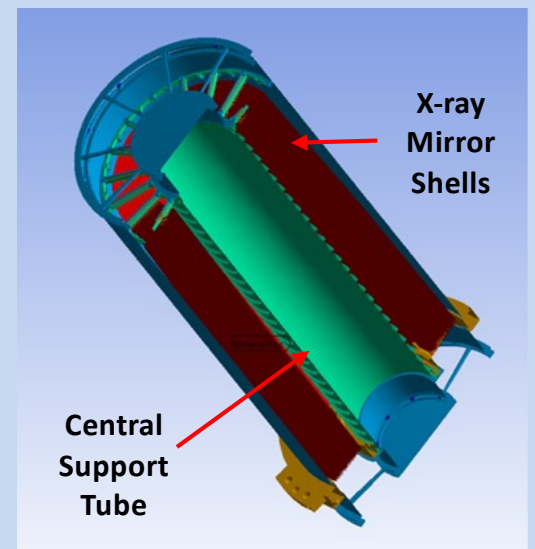
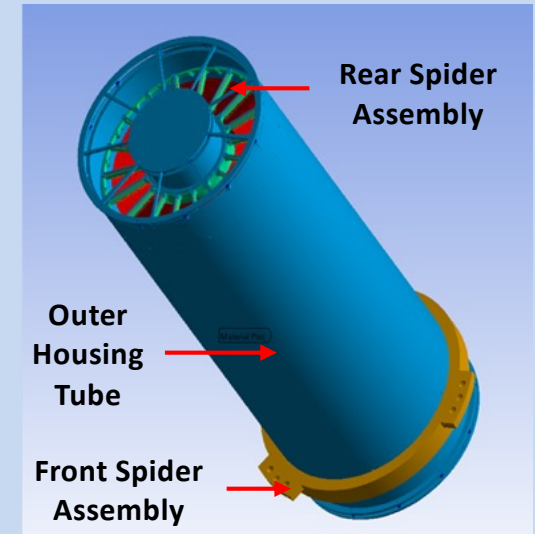
Three IXPE Mirror Module Assemblies



MMA, showing 24 shells

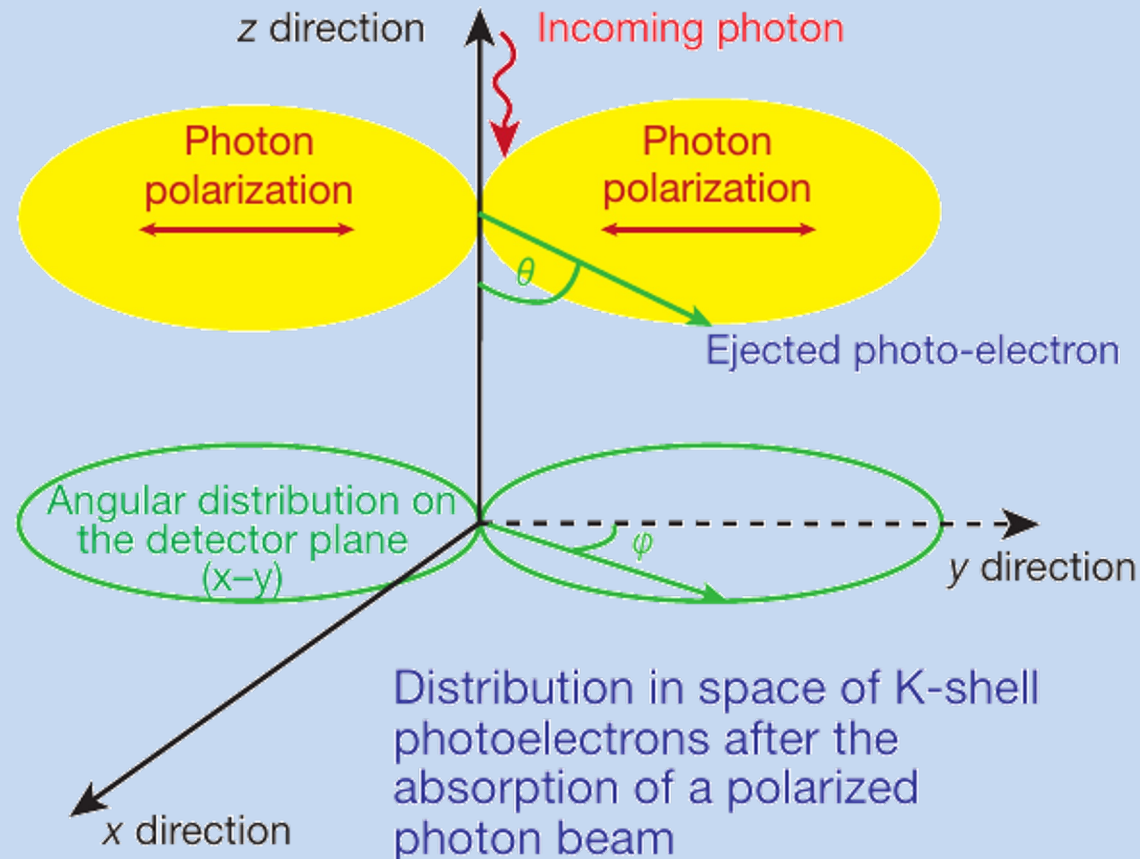


MMA with Thermal Shield on end



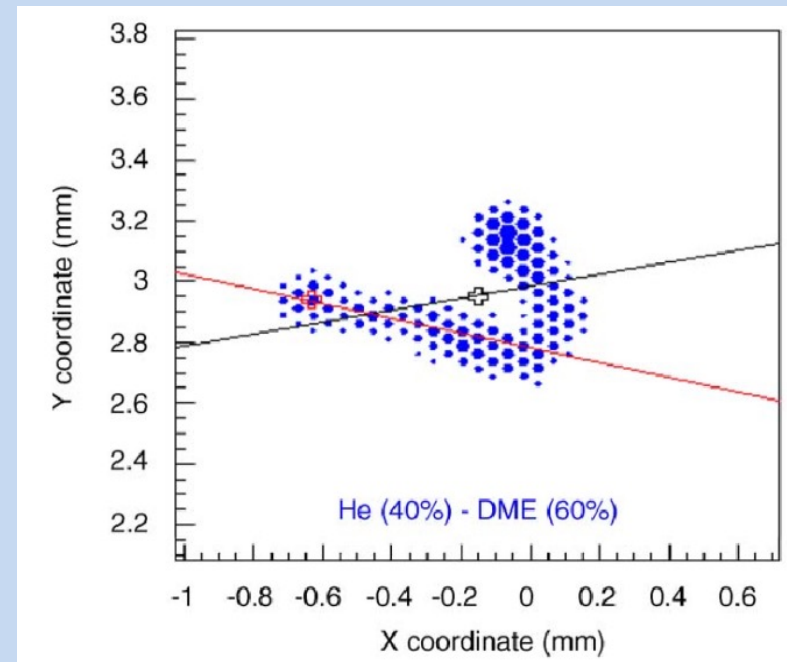
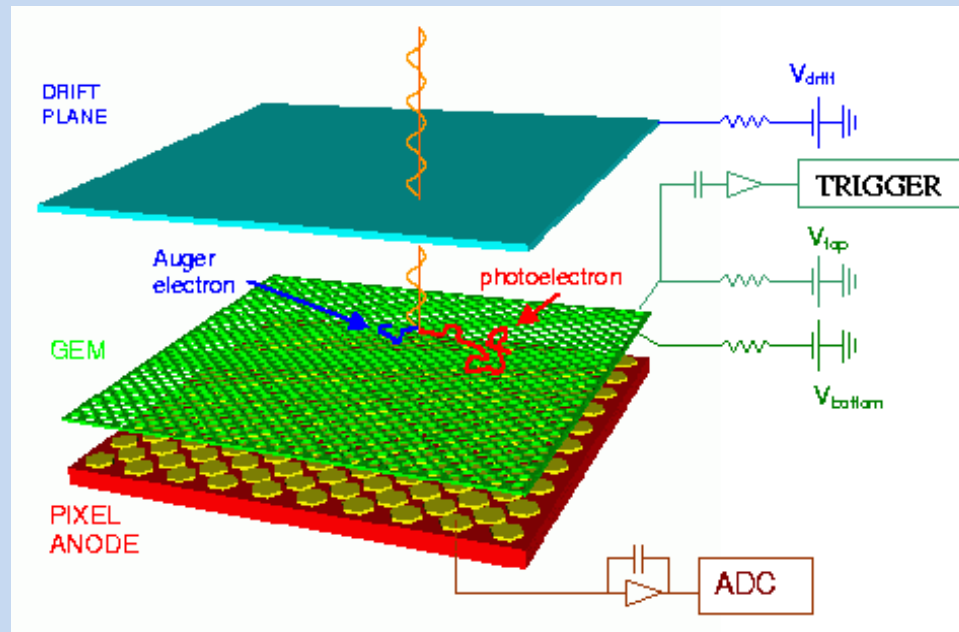
Detection Principle

- The detection principle is based upon the photoelectric effect



$$\frac{d\sigma}{d\Omega} = r_0^2 Z^5 \alpha_0^4 \left(\frac{1}{\beta} \right)^{7/2} 4\sqrt{2} \sin^2 \theta \cos^2 \varphi, \quad \text{where } \beta \equiv \frac{E}{mc^2} = \frac{h\nu}{mc^2}$$

Gas Pixel Detector

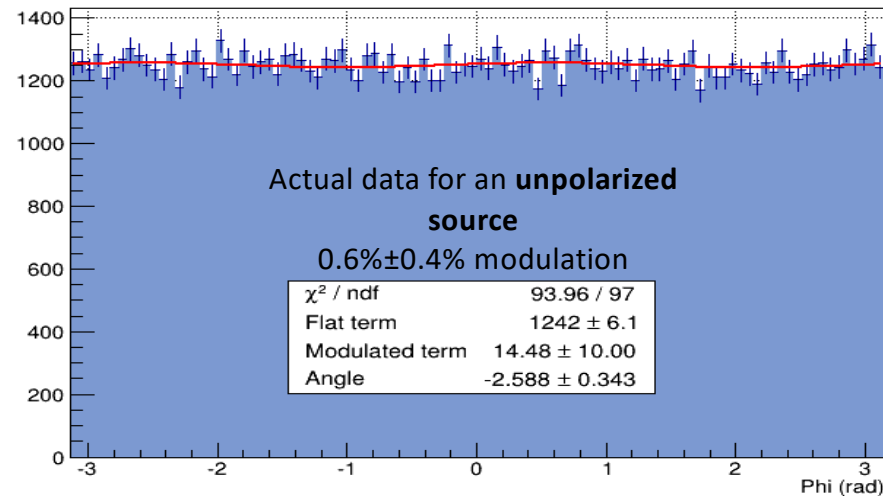
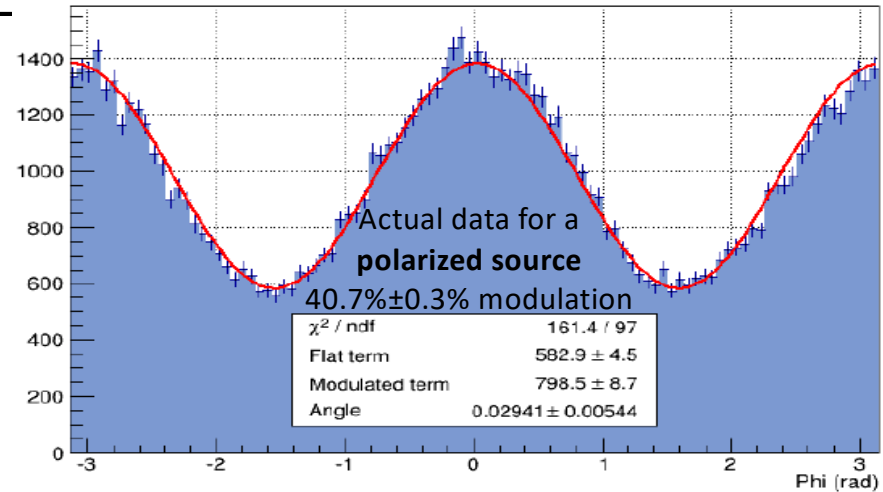
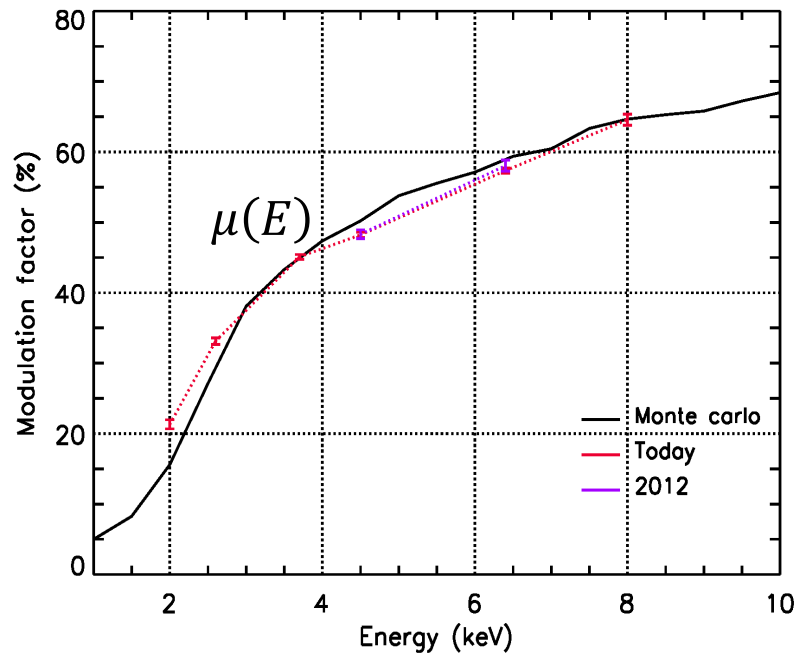


- Include a Filter & Calibration wheel with
 - Filters for specific observations (very bright sources, background)
 - Calibrations sources (polarized and unpolarized, gain)

POLARIZATION FROM MODULATION HISTOGRAM AND CALIBRATED MODULATION FACTOR

- **Polarization degree**

- $\Pi = \text{Modulation} / \mu(E)$



- **Polarization degree**

- $\Pi = \text{Modulation} / \mu(E)$



Targets observed by IXPE in 1st year

1. Accreting X-ray pulsars

Her X-1 (Nature Astronomy)
Cen X-3 (ApJ Letters)
4U 1626-67 (ApJ)
Vela X-1 (ApJ Letters, subm.)
X Per
GX 301-2
GRO J1008-57
EXO 2030+375

2. Accreting non-magnetic neutron stars

GS 1826-238 (ApJ)
Cyg X-2 (MNRAS)
XTE J1701-462 (TOO, in prep.)
4U 1820-30
GX 9+9

3. Magnetar(s)

4U 0142+61 (Science)
1RXS J170849

4. Pulsars/Pulsar Wind Nebulae

Crab (submitted)
Vela (Nature)
PSR B0540-69

5. Supernova remnant(s)

Cas A (ApJ)
Tycho (ApJ, subm.)
SN1006
MSH 15-52

6. Stellar-mass black holes

Cyg X-1 (Science)
4U 1630-47
LMC X-1
Cyg X-3

7. Seyferts and Milky Way BH

MCG-5-23-16 (MNRAS)
Circinus galaxy (MNRAS)
Sgr A cloud (submitted)
IC 4329A

8. Blazars /radio galaxies

Mrk 501 (Nature)
Cen A (ApJ)
Mrk 421 (ApJ)
BL Lac (ApJ Letters)
3C 454.3
3C 273
1ES 1959+65
3C 279

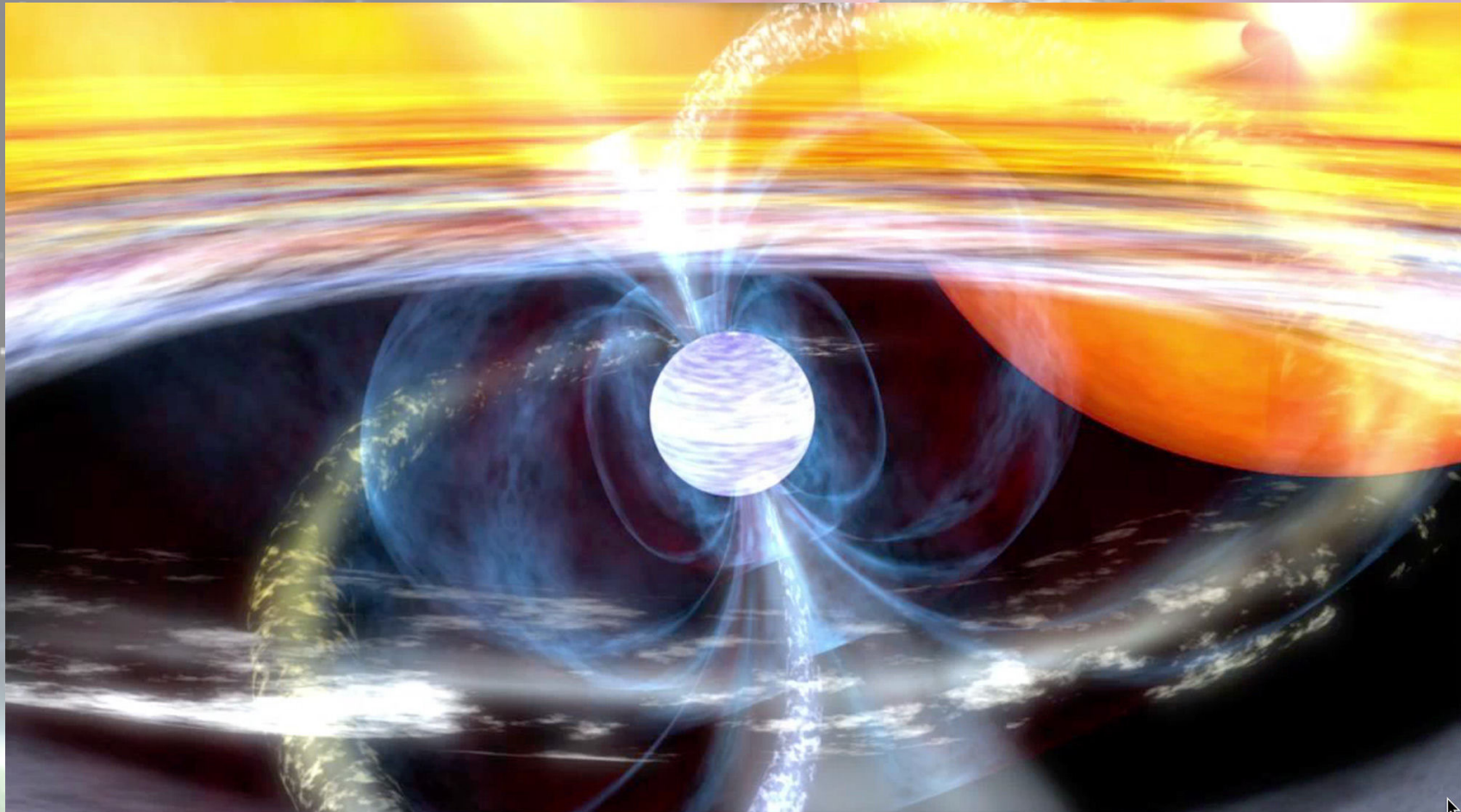
9. Other

GRB 221009A



IXPE
Imaging
X-Ray
Polarimetry
Explorer

Accreting X-ray pulsars

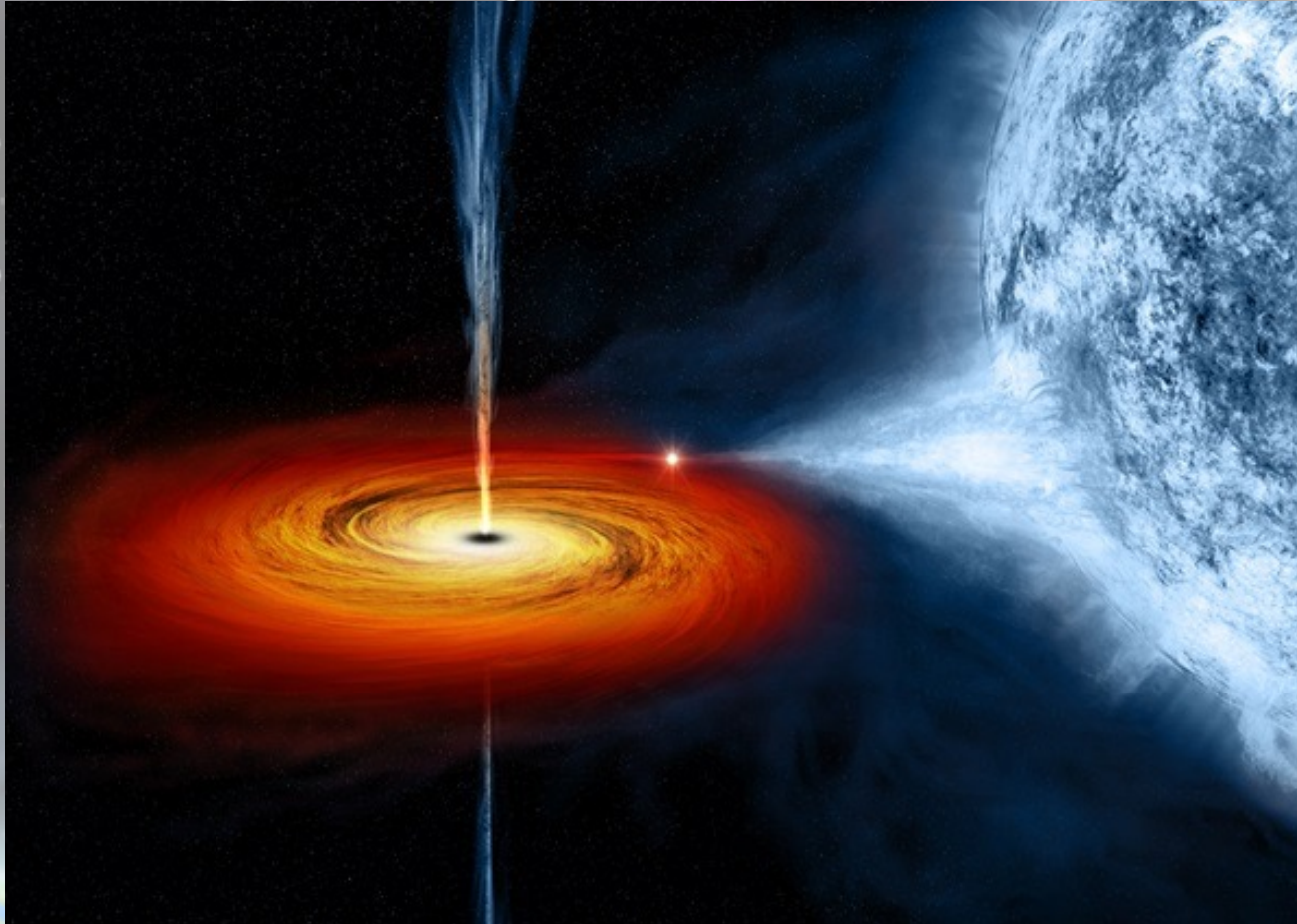


Next talk by Sergey Tsygankov



IXPE
Imaging
X-Ray
Polarimetry
Explorer

Cygnus X-1



Cygnus X-1

$$M_{\text{BH}} = 21.2 \pm 2.2 M_{\odot}$$

$$M_2 = 40.6^{+7.7}_{-7.1} M_{\odot}$$

$$P = 5.6 \text{ days}$$

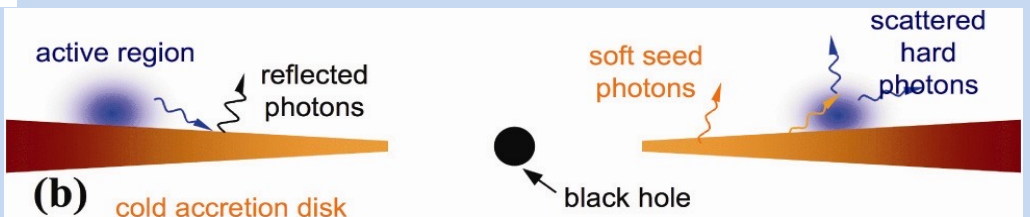
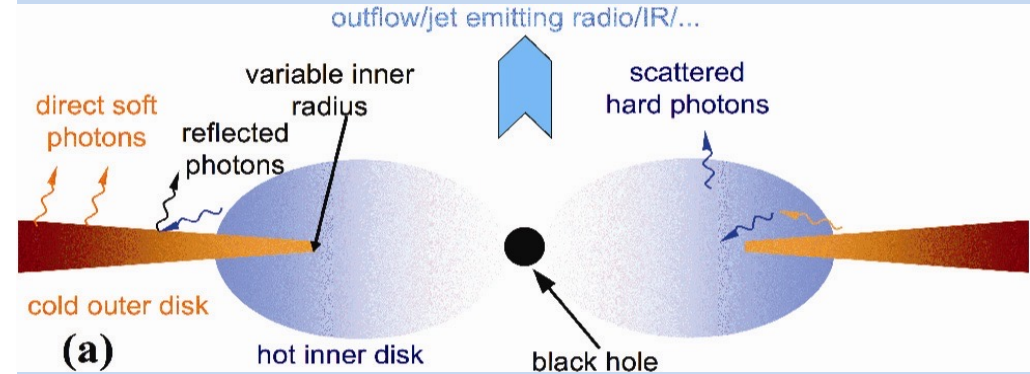
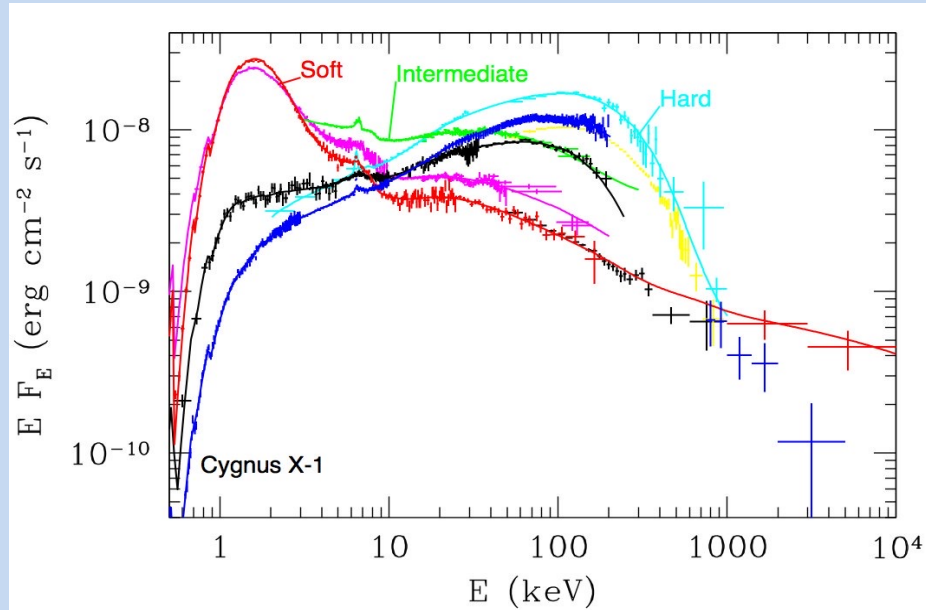
$$d = 2.22^{+0.18}_{-0.17} \text{ kpc}$$

Orbital inclination:

$$i = 27.51^{+0.8}_{-0.7} \text{ degrees}$$

Miller-Jones et al. 2021

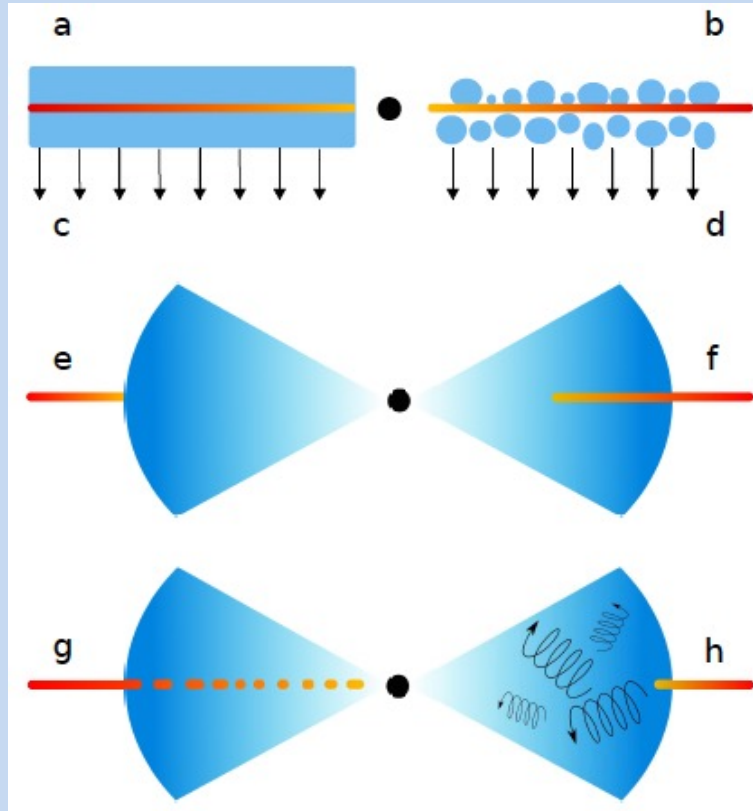
Cygnus X-1 spectra



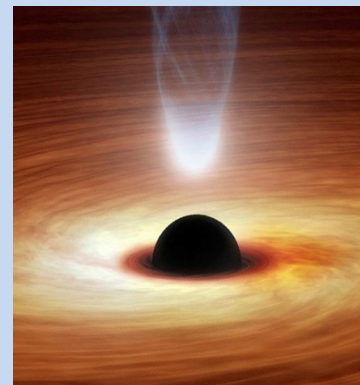
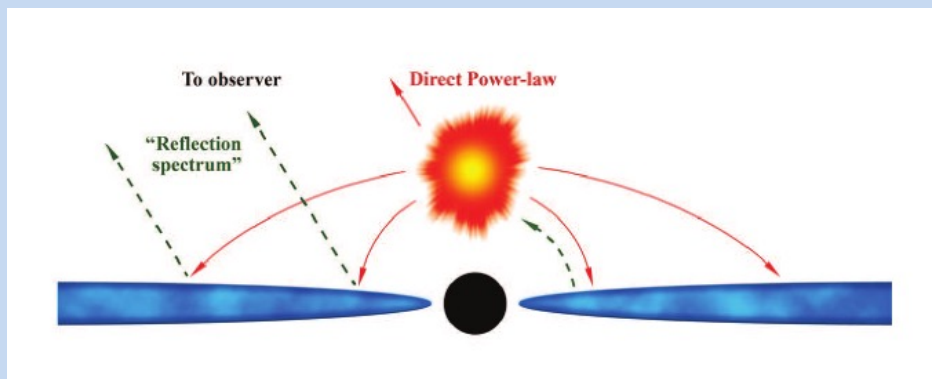
Hard state - standard cold outer disc + hot inner flow

Soft state - standard accretion disc plus nonthermal corona

Cygnus X-1 hard state geometry

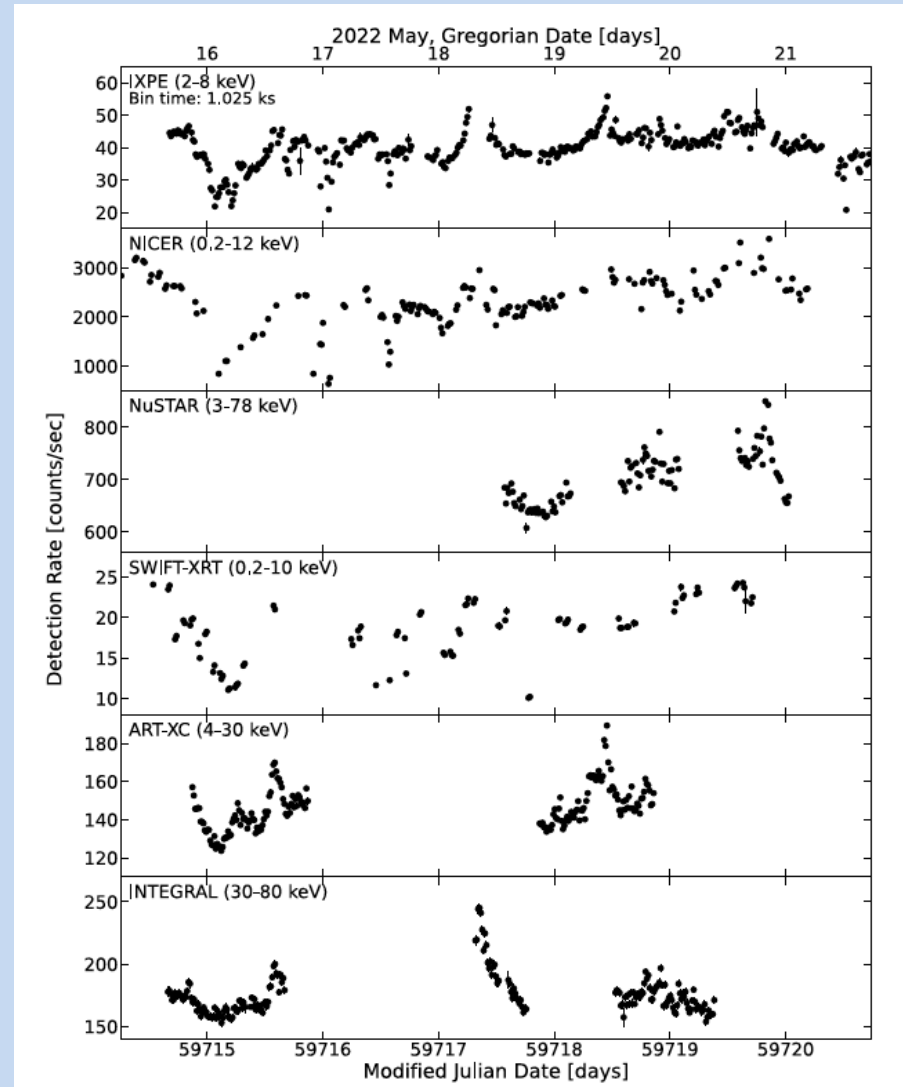


- The hard state spectrum is produced by multiply Compton scattering (thermal Comptonization)
- Polarization is sensitive to the geometry of the "corona", its dynamics and source of seed photons



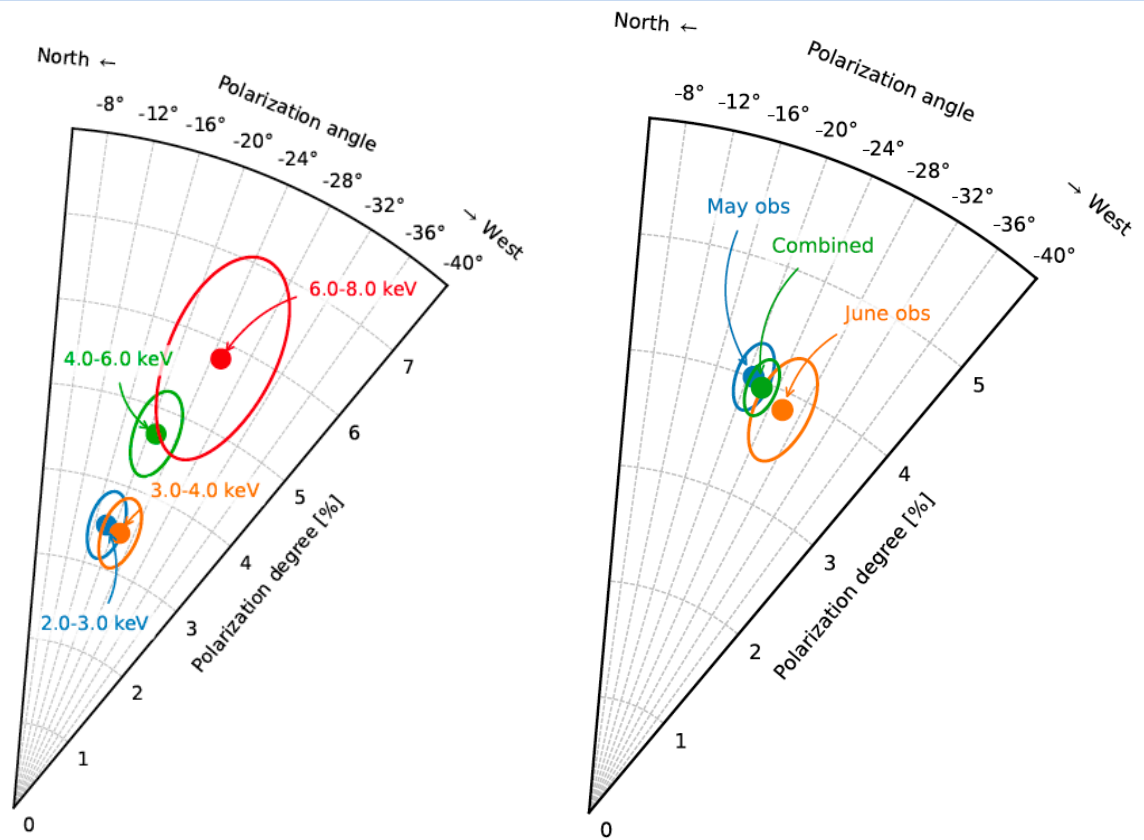
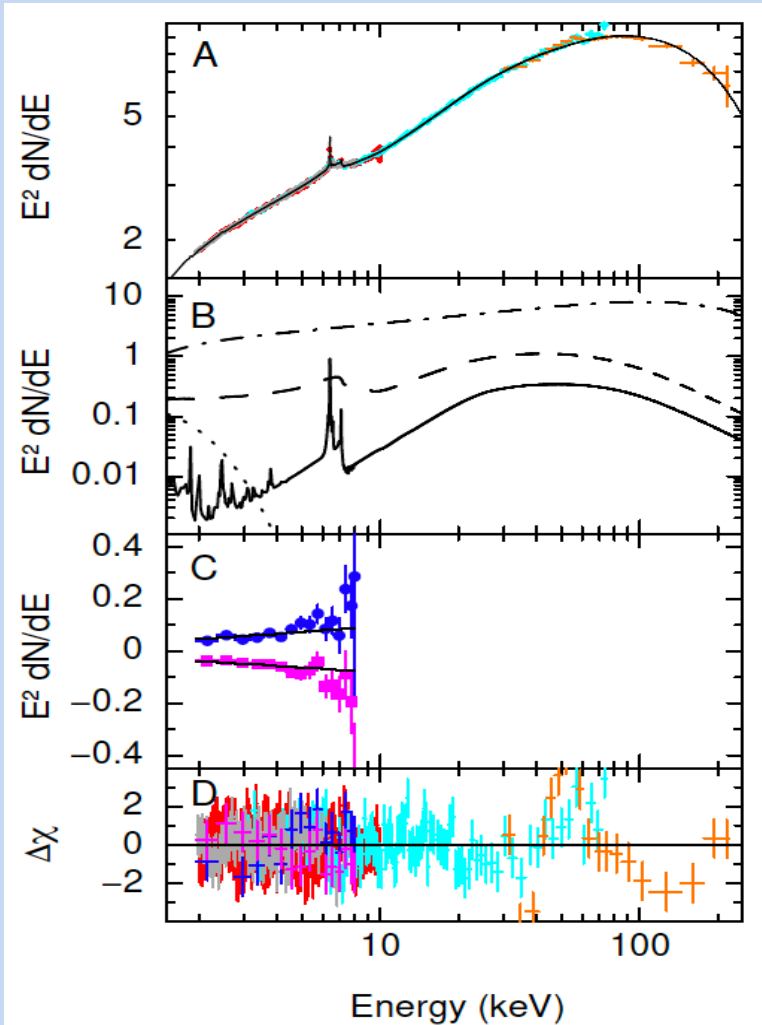
Cygnus X-1 variability

- The source was observed by IXPE in May and June 2022.
- Was also observed by NICER, Nustar, Swift, SRG/ART-XC and INTEGRAL.

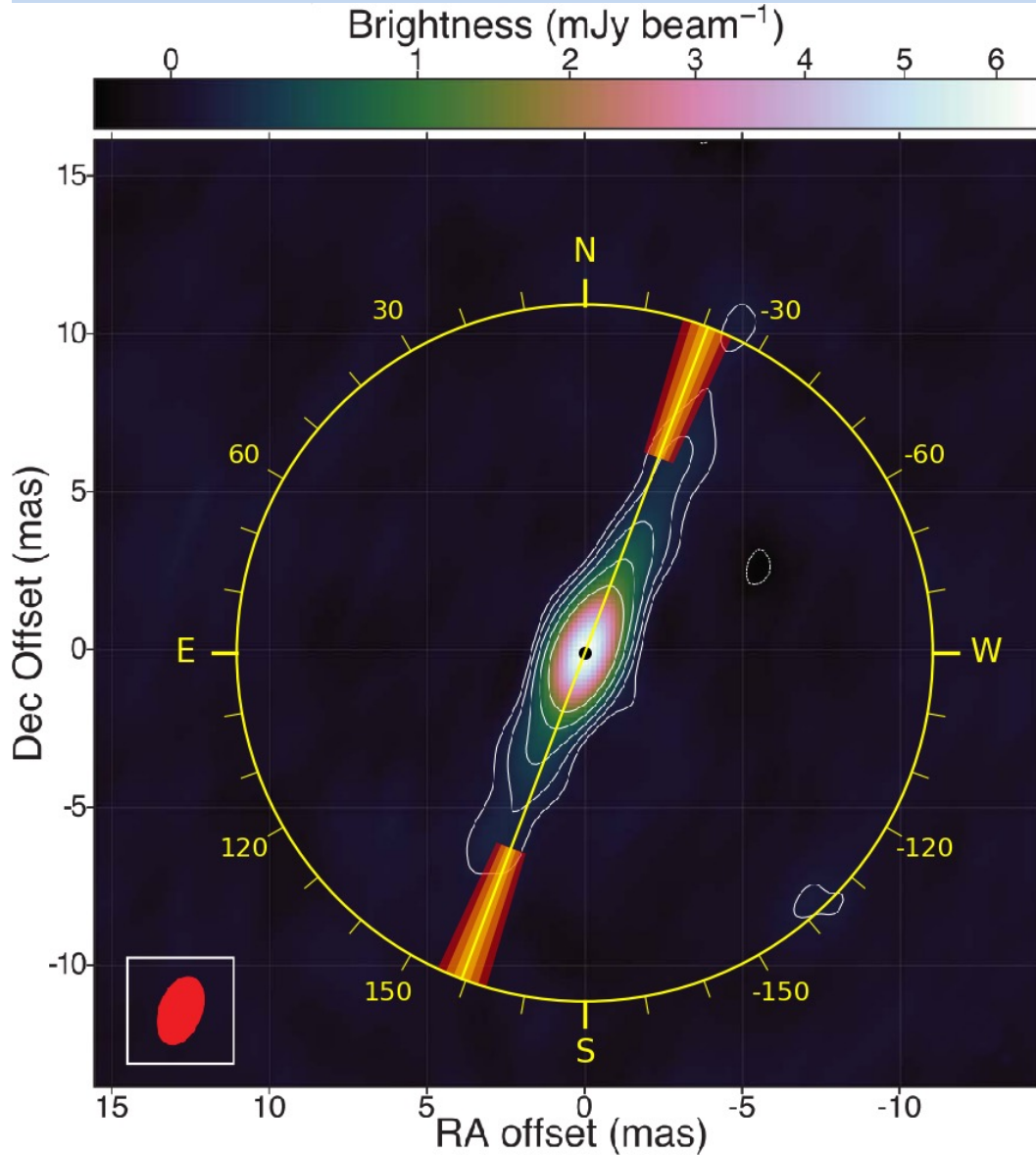


Cygnus X-1

- IXPE observed the source in May and June 2022.
- Cyg X-1 was in the hard state



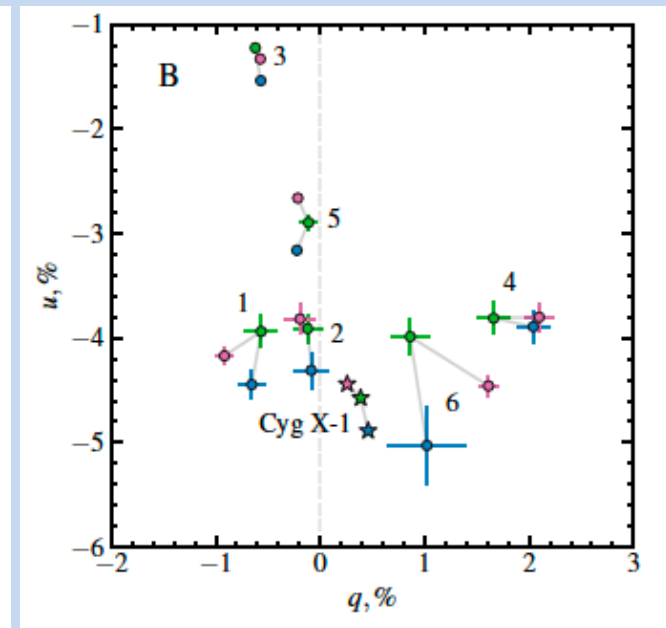
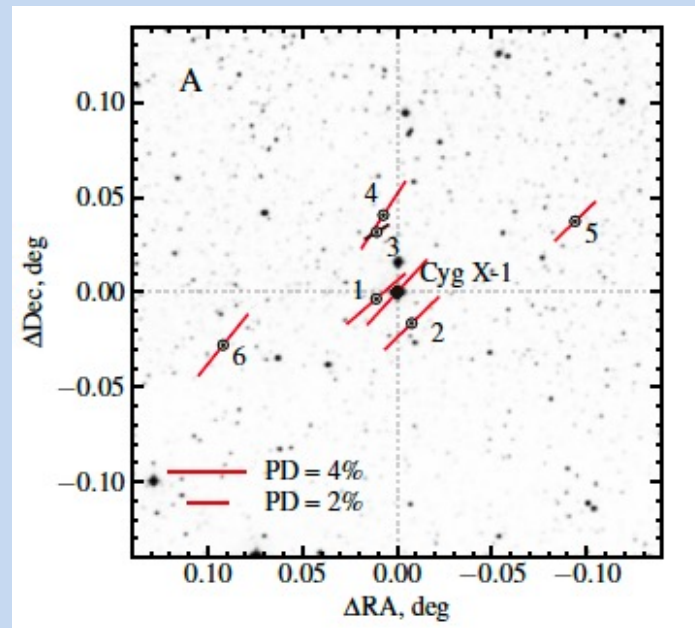
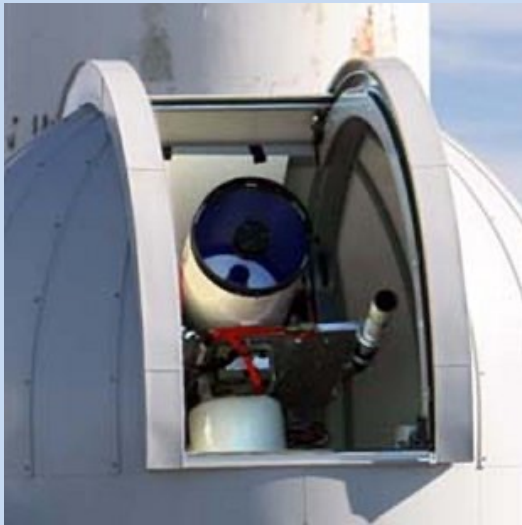
Cygnus X-1



X-ray polarization
parallel to the jet.

Optical polarimetry

- Cygnus X-1 was observed with DIPol-2 polarimeter at T60 Tohoku Univ. Telescope at Haleakala and with Robopol in Creete.**





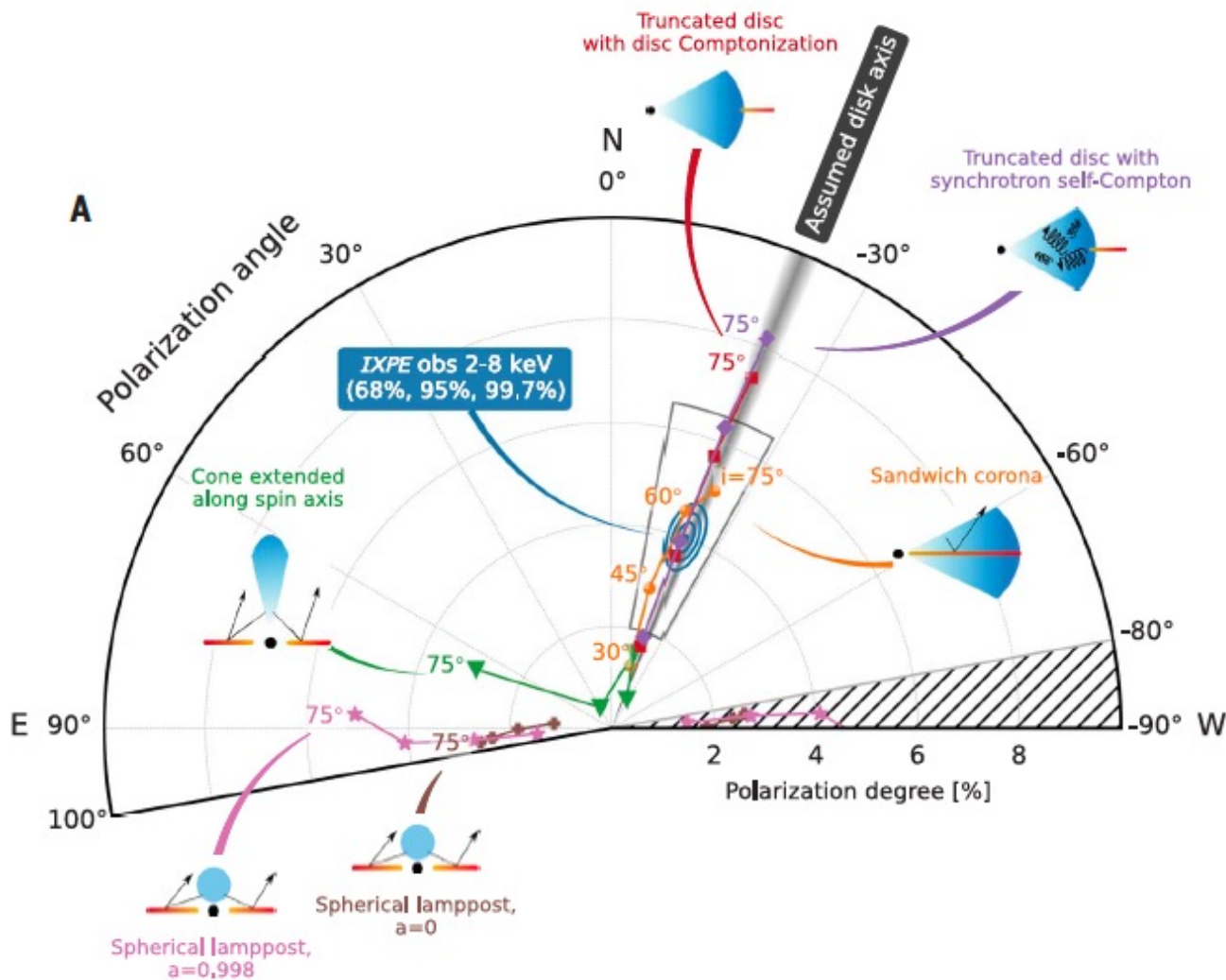
Optical polarimetry

- Cygnus X-1 was observed with DIPol-2 polarimeter at T60 Tohoku Univ. Telescope at Haleakala.

Band	<i>B</i>		<i>V</i>		<i>R</i>	
	<i>q</i> (%)	<i>u</i> (%)	<i>q</i> (%)	<i>u</i> (%)	<i>q</i> (%)	<i>u</i> (%)
Observed polarization of Cyg X-1						
DIPol-2	0.46 ± 0.06	-4.89 ± 0.04	0.39 ± 0.04	-4.57 ± 0.04	0.26 ± 0.03	-4.44 ± 0.03
RoboPol	-	-	-	-	0.61 ± 0.13	-4.74 ± 0.12
Interstellar polarization						
Ref 2/DIPol-2	-0.09 ± 0.17	-4.31 ± 0.17	-0.12 ± 0.14	-3.91 ± 0.14	-0.19 ± 0.15	-3.82 ± 0.15
Ref 1+2/DIPol-2	-0.41 ± 0.11	-4.39 ± 0.11	-0.33 ± 0.10	-3.92 ± 0.10	-0.67 ± 0.07	-4.05 ± 0.07
Ref 2/RoboPol	-	-	-	-	0.39 ± 0.16	-4.00 ± 0.08
Intrinsic polarization of Cyg X-1						
Ref 2/DIPol-2	0.55 ± 0.17	-0.58 ± 0.17	0.51 ± 0.14	-0.66 ± 0.14	0.45 ± 0.15	-0.62 ± 0.15
Ref 1+2/DIPol-2	0.87 ± 0.11	-0.50 ± 0.11	0.72 ± 0.10	-0.65 ± 0.10	0.93 ± 0.07	-0.39 ± 0.07
Ref 2/RoboPol	-	-	-	-	0.22 ± 0.21	-0.74 ± 0.14
Intrinsic polarization of Cyg X-1						
	PD (%)	PA (deg)	PD (%)	PA (deg)	PD (%)	PA (deg)
Ref 2/DIPol-2	0.79 ± 0.17	-23 ± 6	0.83 ± 0.14	-26 ± 5	0.77 ± 0.15	-27 ± 6
Ref 1+2/DIPol-2	1.00 ± 0.11	-15 ± 3	0.97 ± 0.10	-21 ± 3	1.01 ± 0.07	-11 ± 2
Ref 2/RoboPol	-	-	-	-	0.77 ± 0.15	-37 ± 6

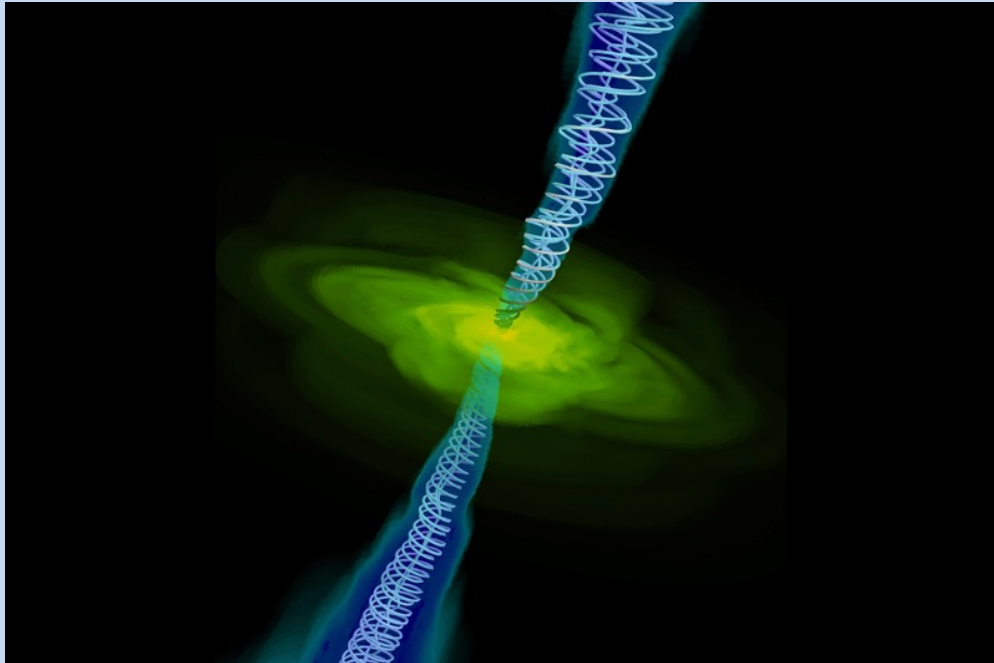
IXPE Cygnus X-1: polarization from Comptonization in different geometries

Imaging
X-Ray
Polarimetry
Explorer

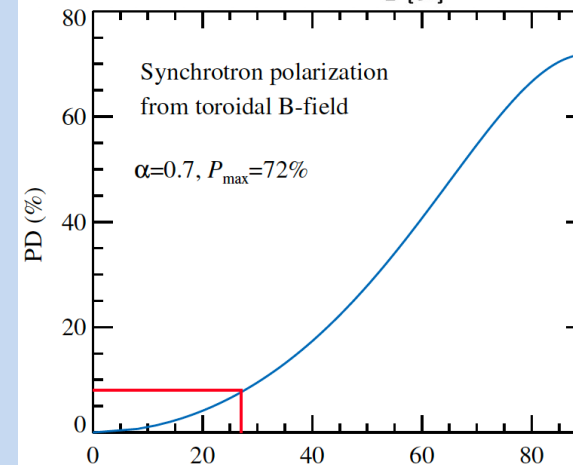
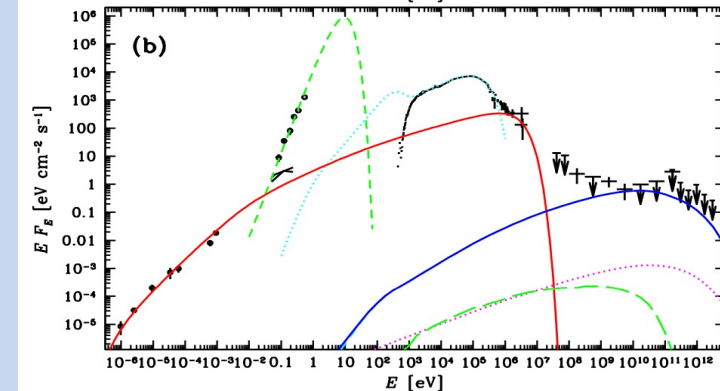
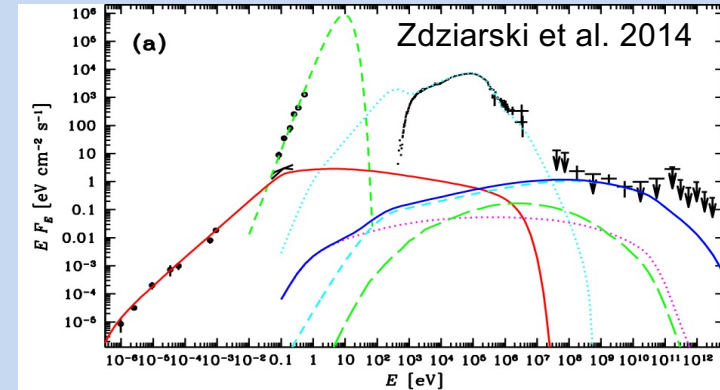


- Models of a jet or a lamppost are rejected.
- Hot flow or slab-corona are preferred, but slab-corona produces too soft spectra.
- Inclination of 40-45 deg is needed. Misalignment perpendicular to the sky plane?

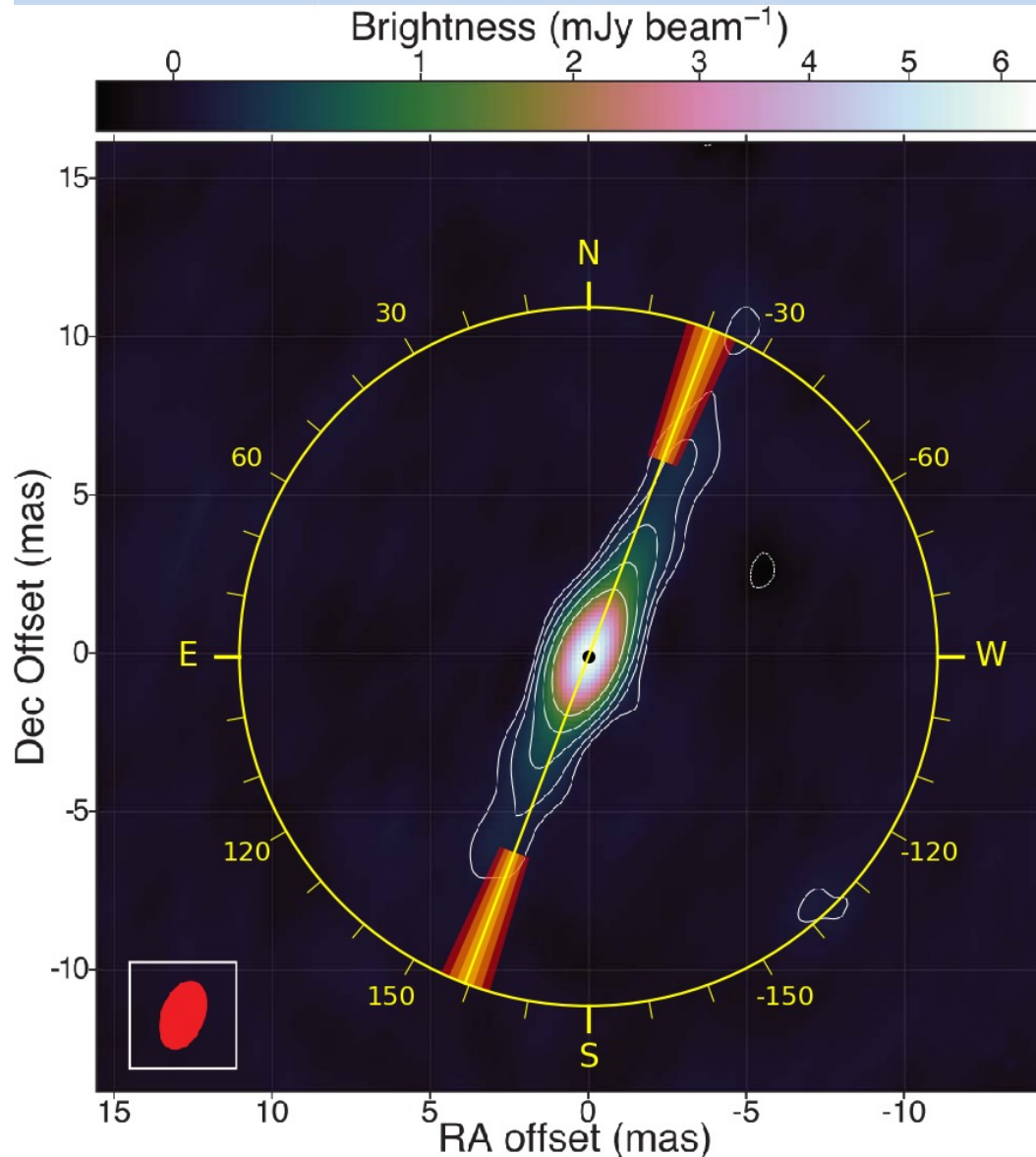
Cygnus X-1: synchrotron from the jet?



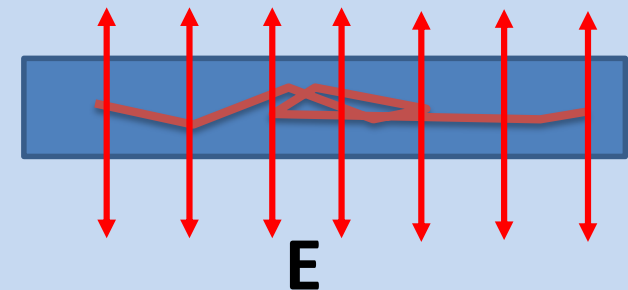
- Synchrotron emission \rightarrow high pol. degree
- Synchrotron is unlikely to contribute more than 5% of flux; $\ll 4\%$ pol. degree.
- Polarization \parallel jet \rightarrow Toroidal magnetic field is needed.



Cygnus X-1



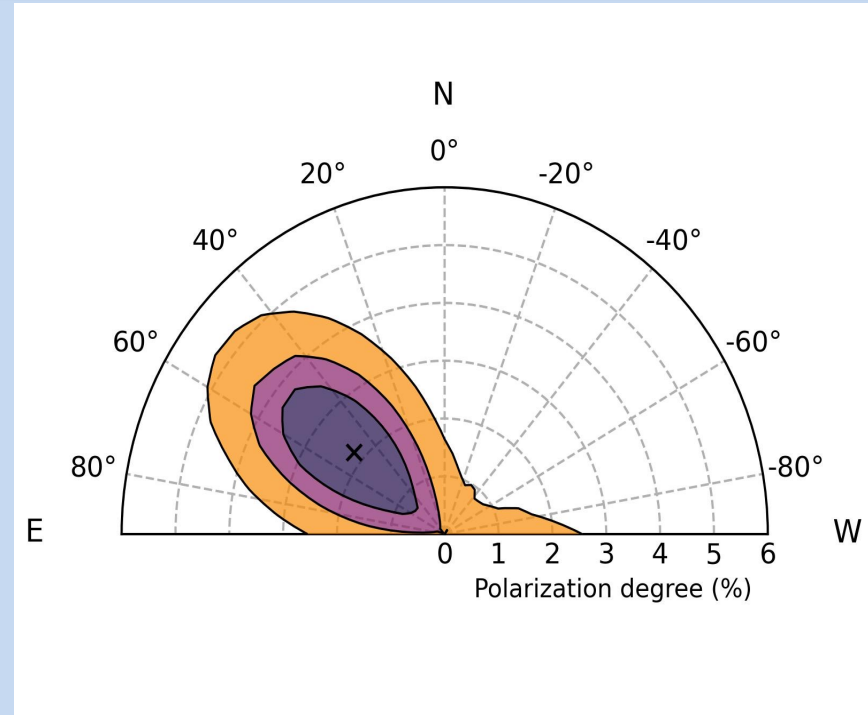
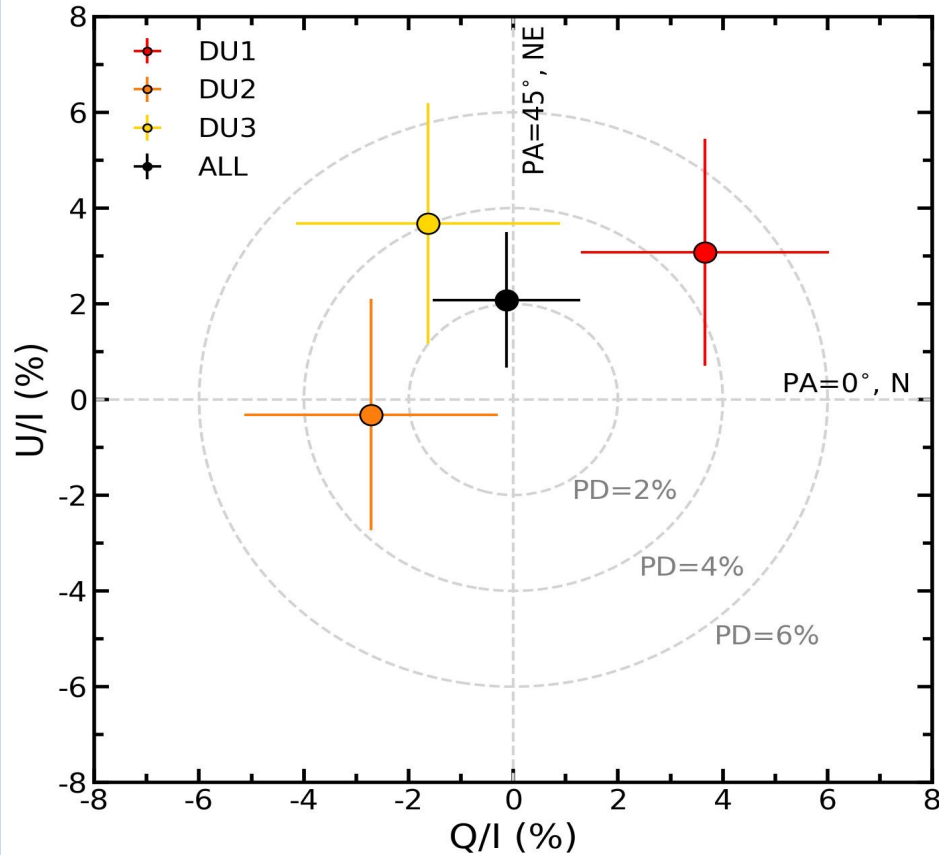
- X-ray polarization parallel to the jet \Rightarrow X-ray emitting region is perpendicular to the jet.



Polarization is perpendicular to the disk. Scattering produces polarization normal to the scattering plane

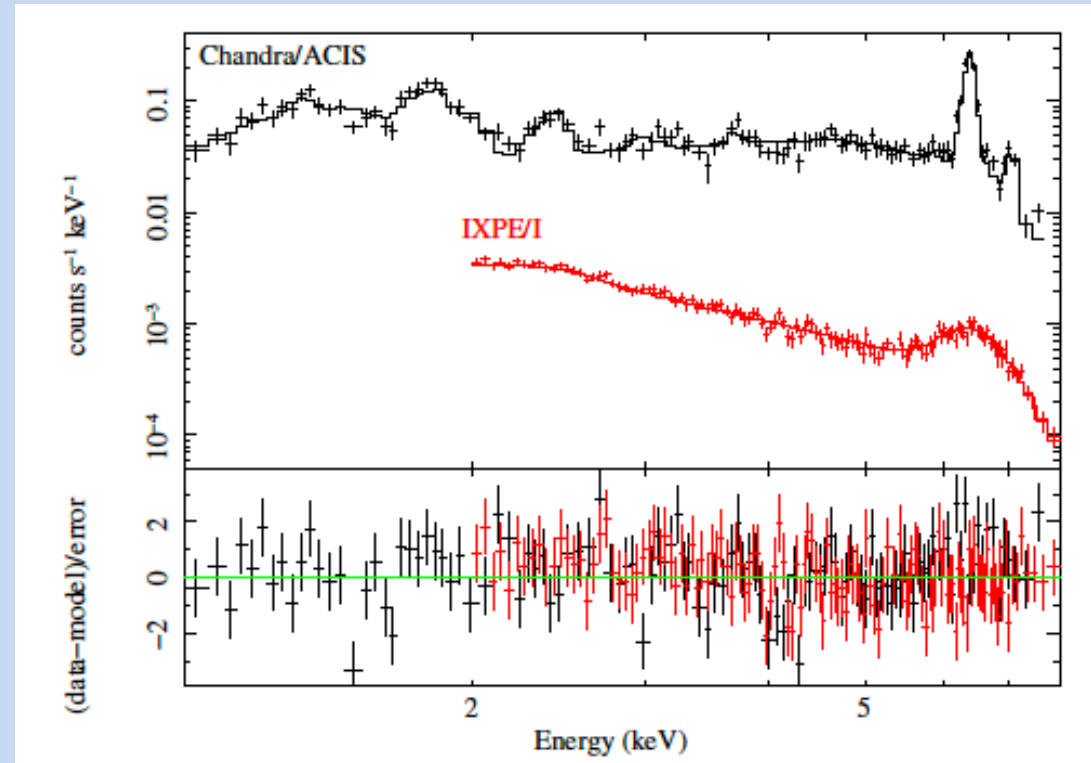
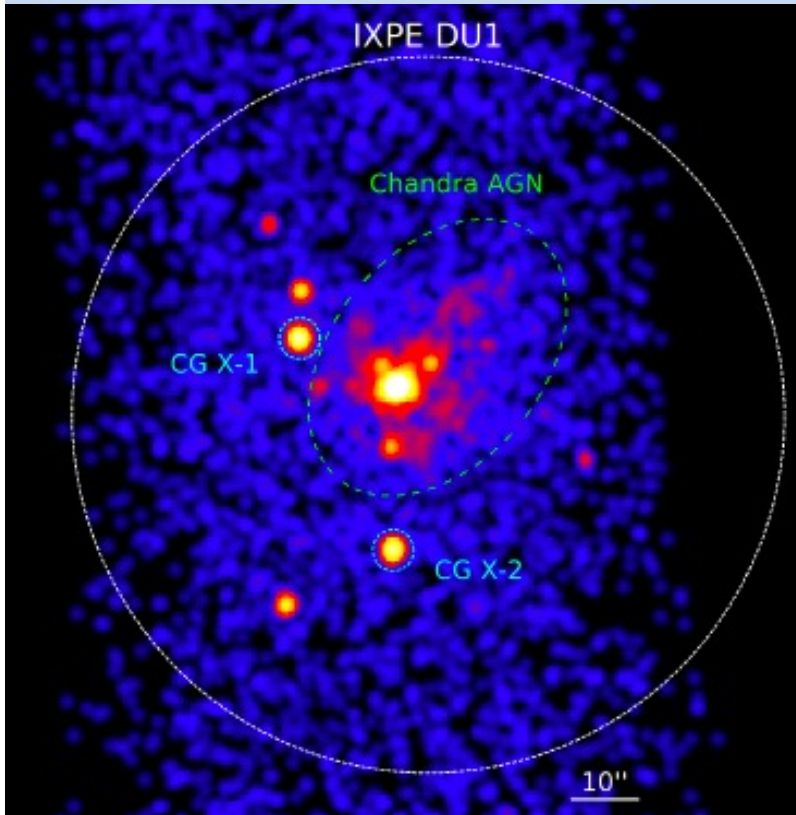
- Optical (intrinsic) polarization has the same angle \Rightarrow orbit perpendicular to the jet.
- How to get 4% polarization?

MGC -5-23-16 (Seyfert 1)



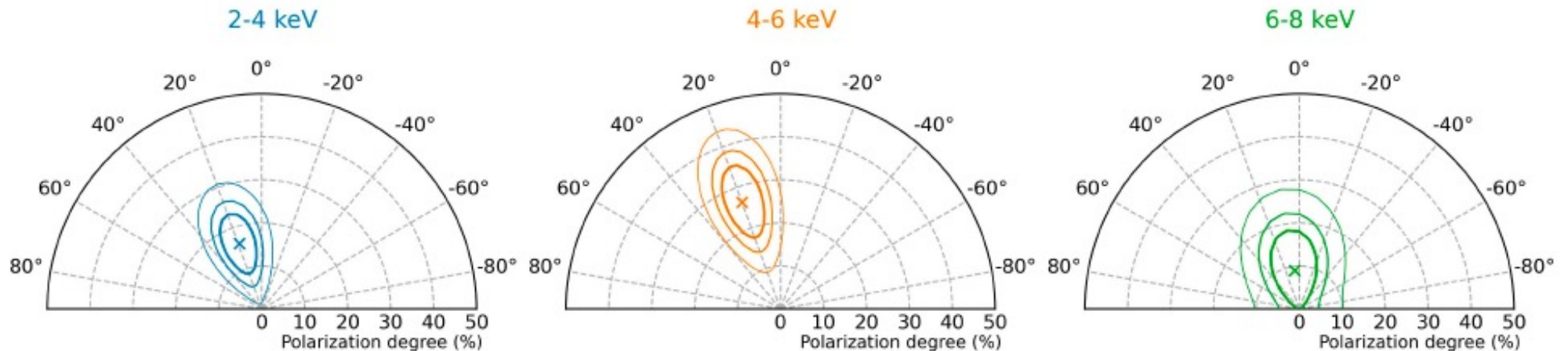
- Upper limit to the polarization degree of 4.7% is found.
- Highly inclined ($>50^\circ$) slab geometries can be ruled out.

Circinus galaxy (Seyfert 2)

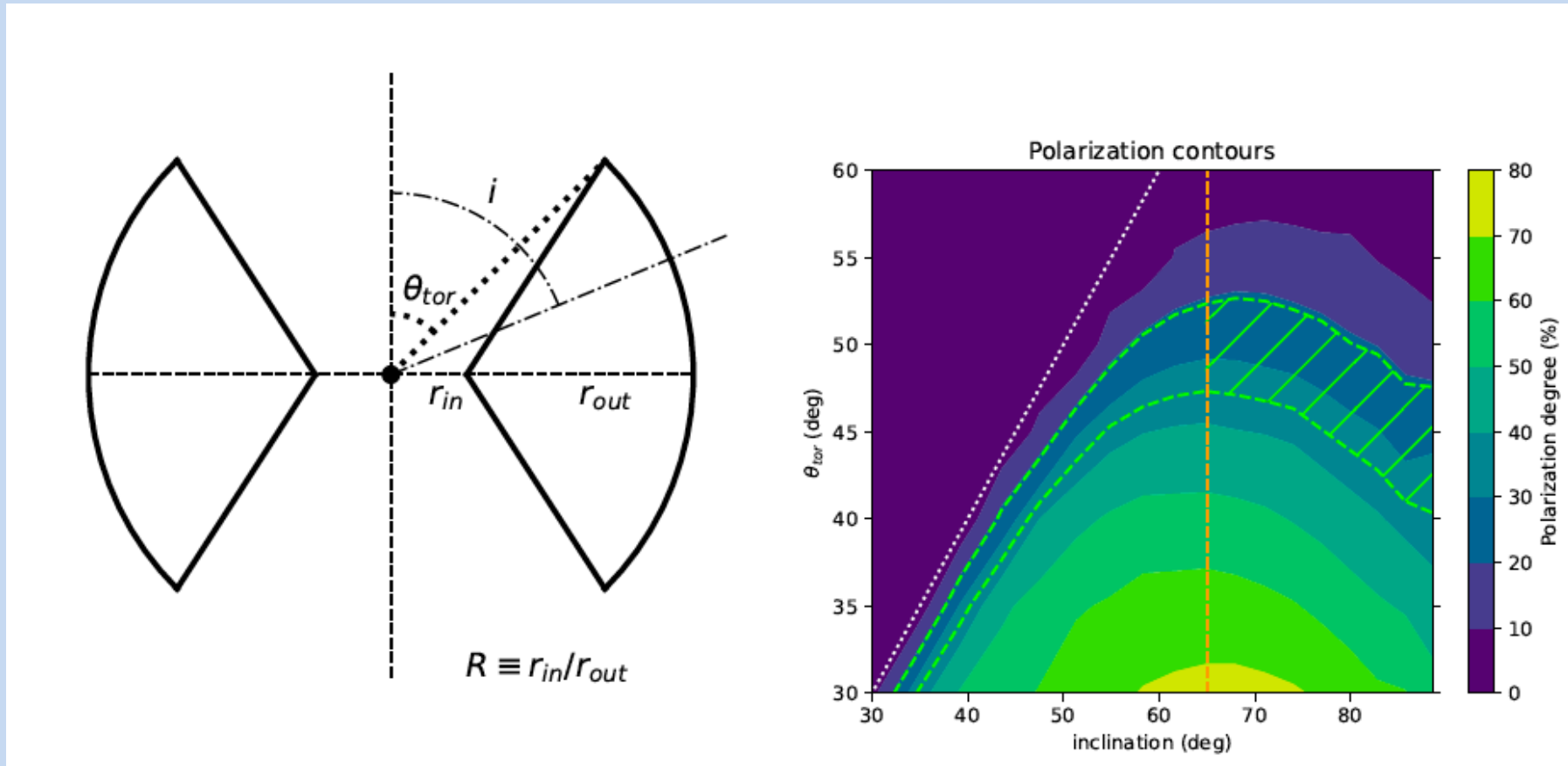


Circinus galaxy

Energy	P.D. (%)	P.A. (deg)
2–8 keV	17.6 ± 3.2	16.9 ± 5.3
2–4 keV	16.0 ± 4.9	19.1 ± 8.9
4–6 keV	26.3 ± 5.7	20.2 ± 7.5
2–6 keV	20.0 ± 3.8	19.1 ± 5.5
6–8 keV	< 24.5	-

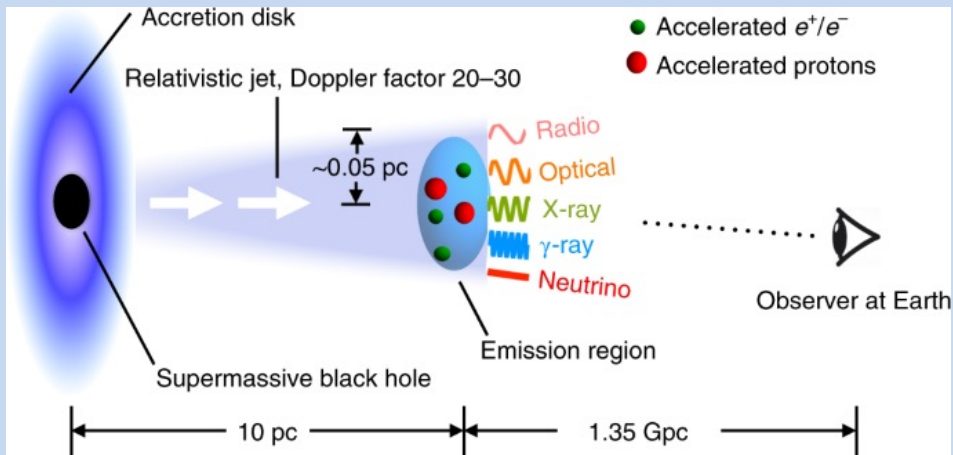


Circinus galaxy

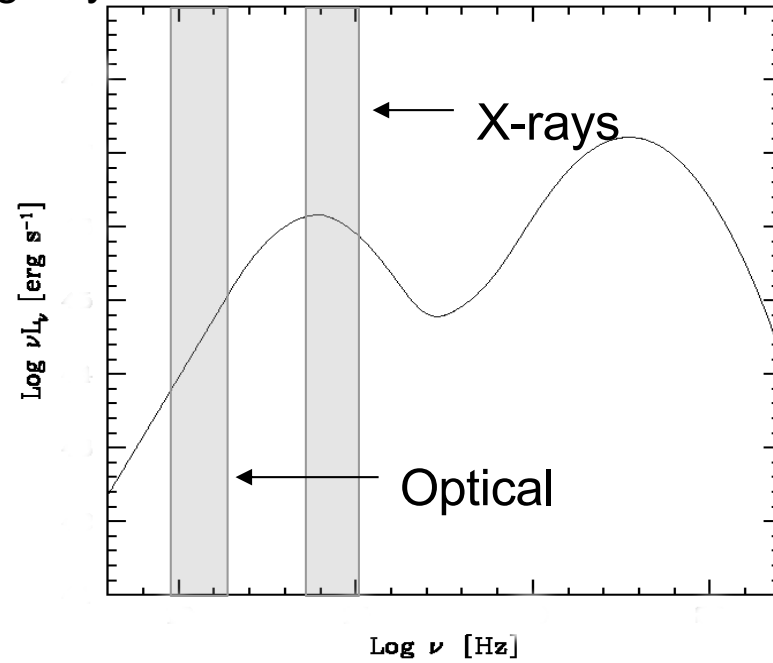


Single scattering by a toroidal surface gives 25% polarization for 45 deg opening angle of the torus and 65 deg inclination.

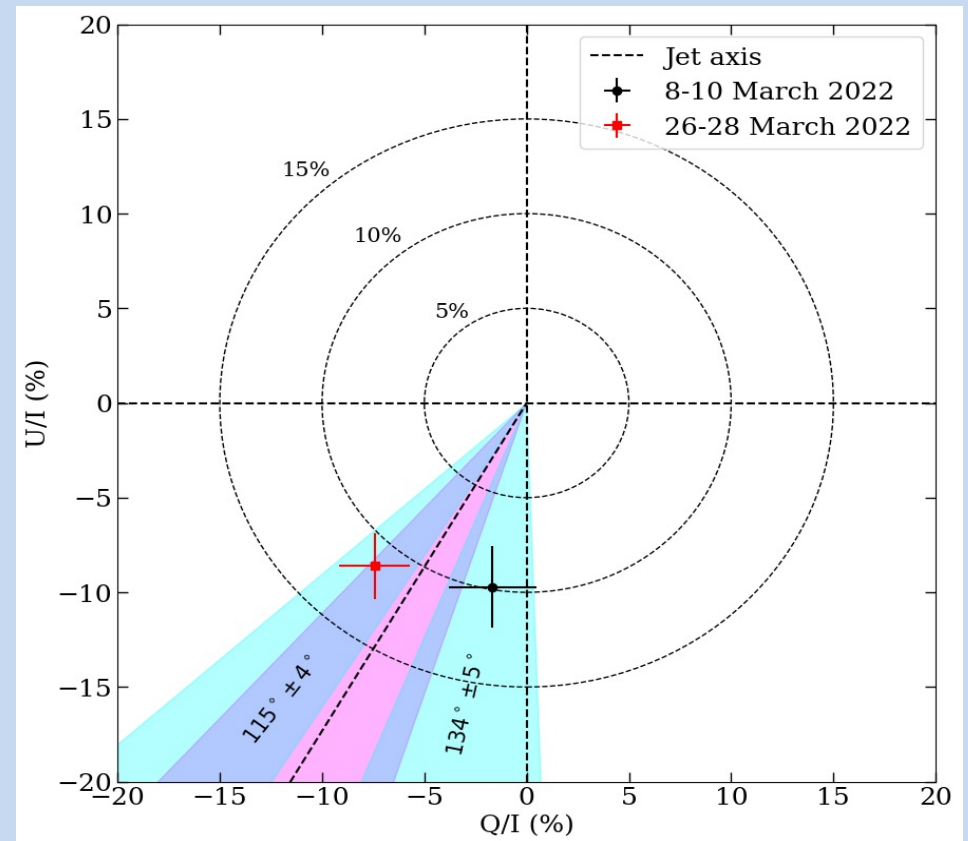
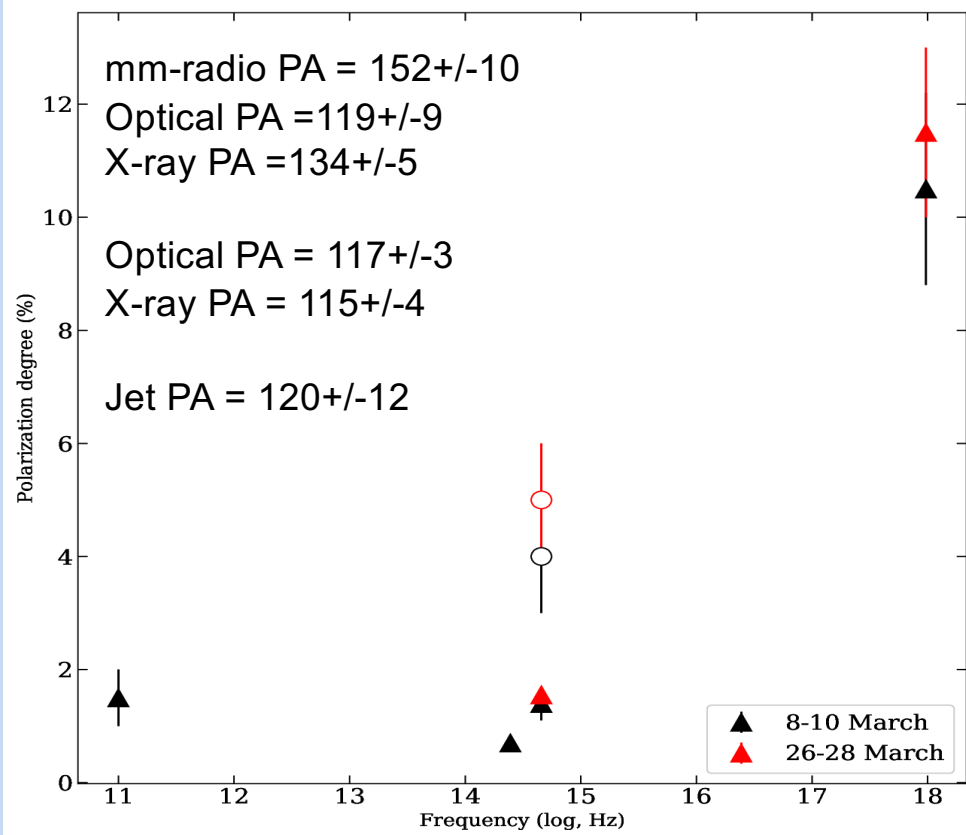
Blazars



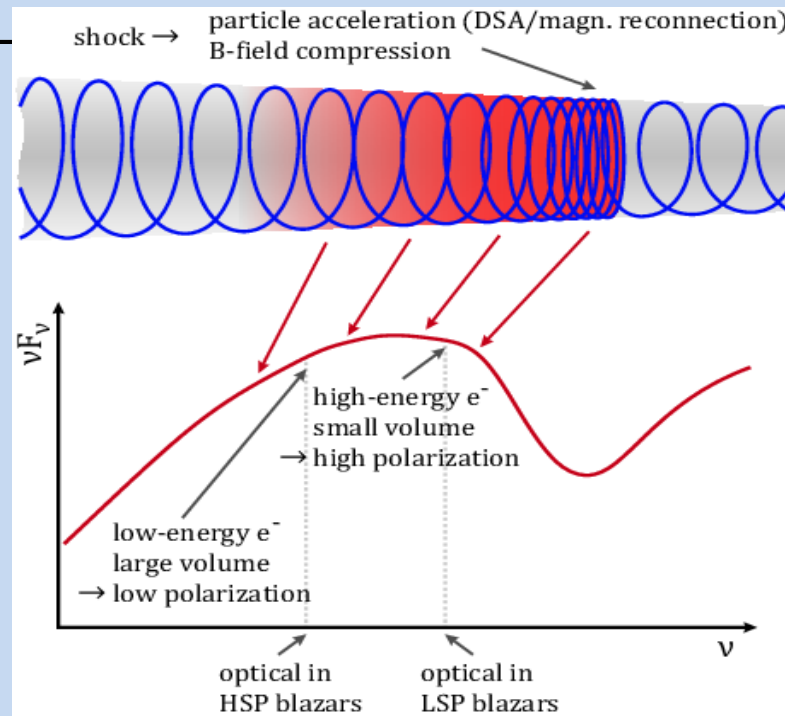
High Synchrotron Peaked



Blazars: the case of Mrk 501

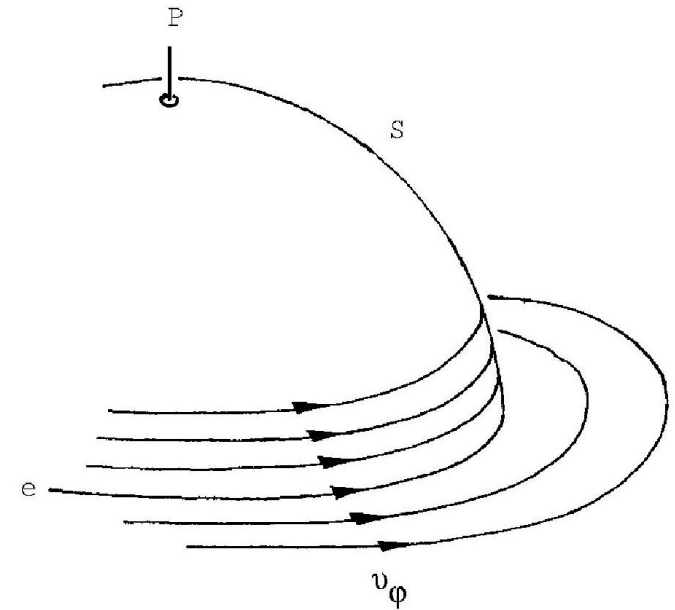
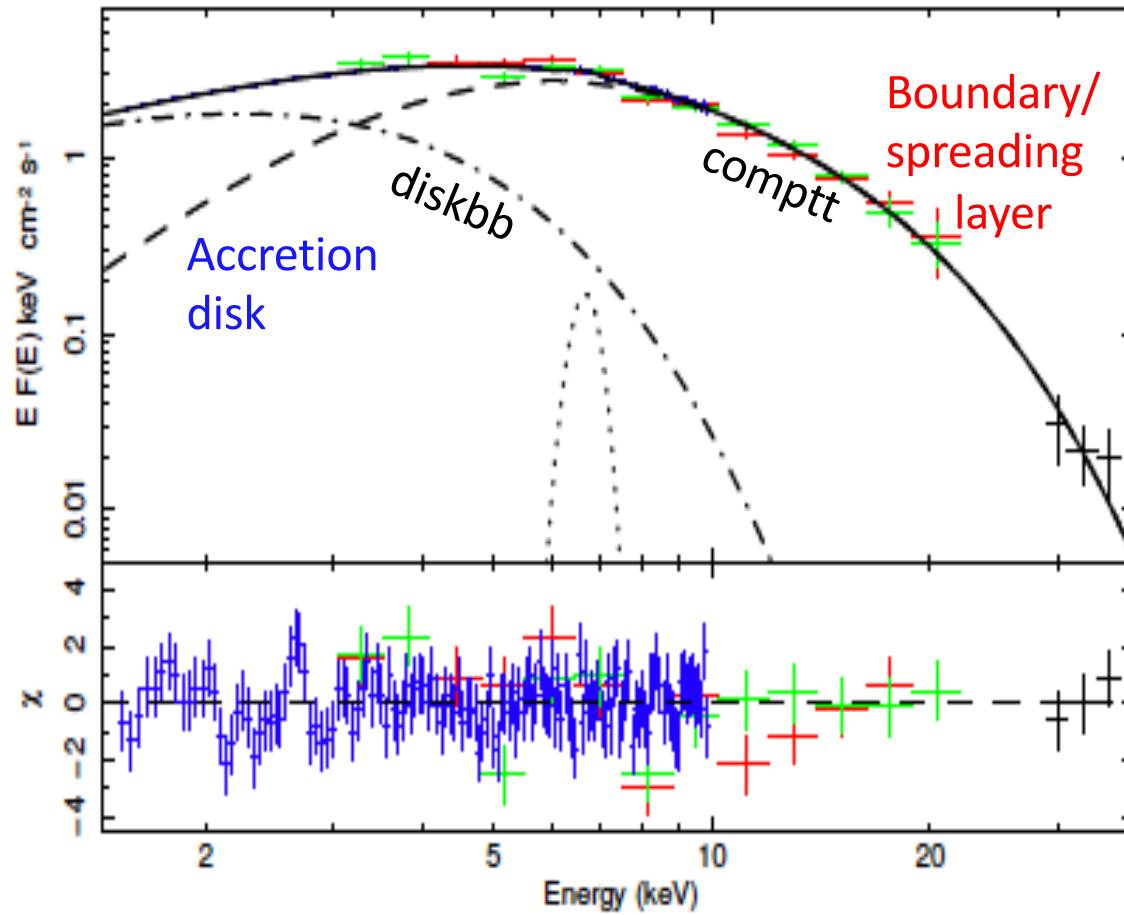


Blazars



Model	Multiwavelength polarization	Variability [†]	Polarization angle
Single zone	constant*	moderate	any
Multizone	mildly chromatic	high	any
Energy stratified (shock)	strongly chromatic	slow	along the jet axis
Energy stratified (magnetic reconnection)	constant	moderate	perpendicular to jet axis
Observed	strongly chromatic	slow	along the jet axis

Nonmagnetic NS: Cyg X-2



Nonmagnetic NS: Cyg X-2

IXPE: $PD=1.8\pm0.3\%$ at $PA=140\pm4$ deg

OSO-8 (1976-1980):

$PD=5.0\pm1.8\%$ at $PA=138\pm10$ deg

Radio jet: $PA=141$ deg

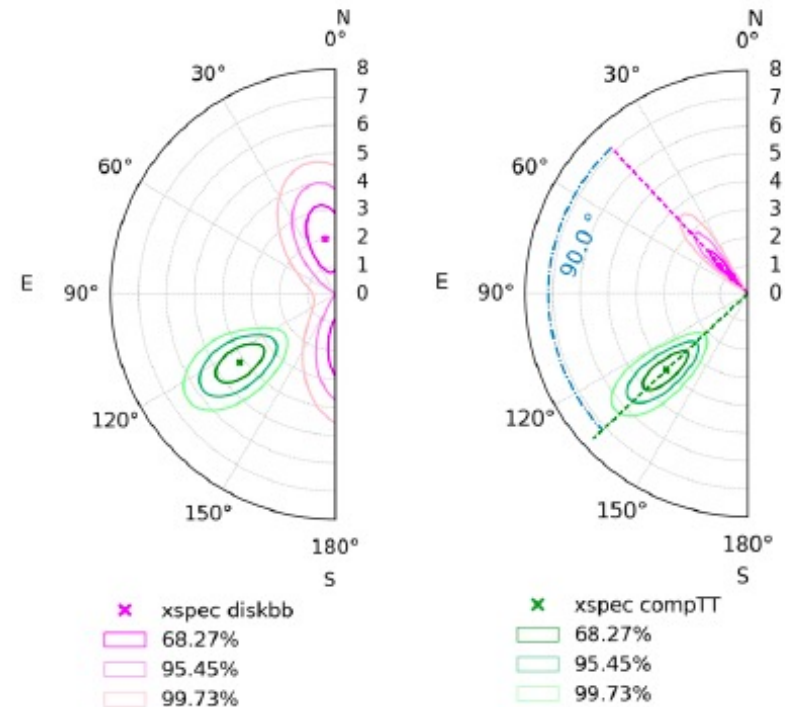
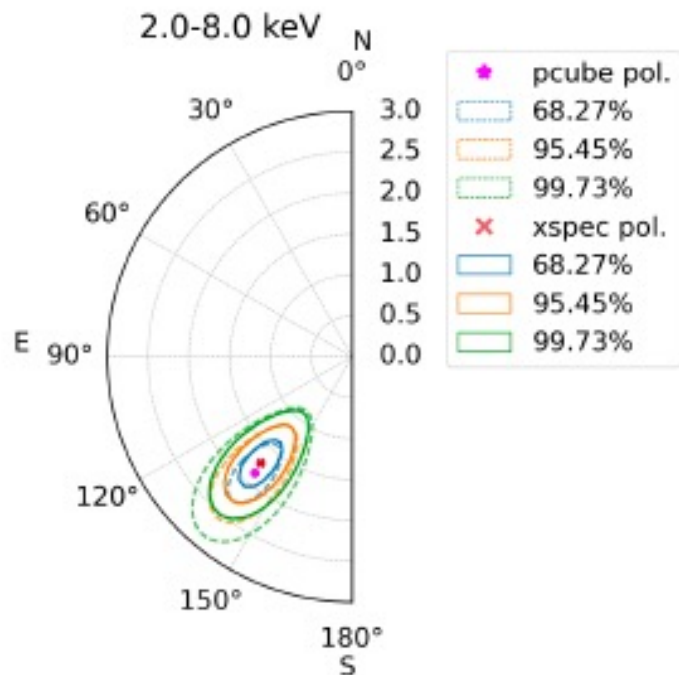
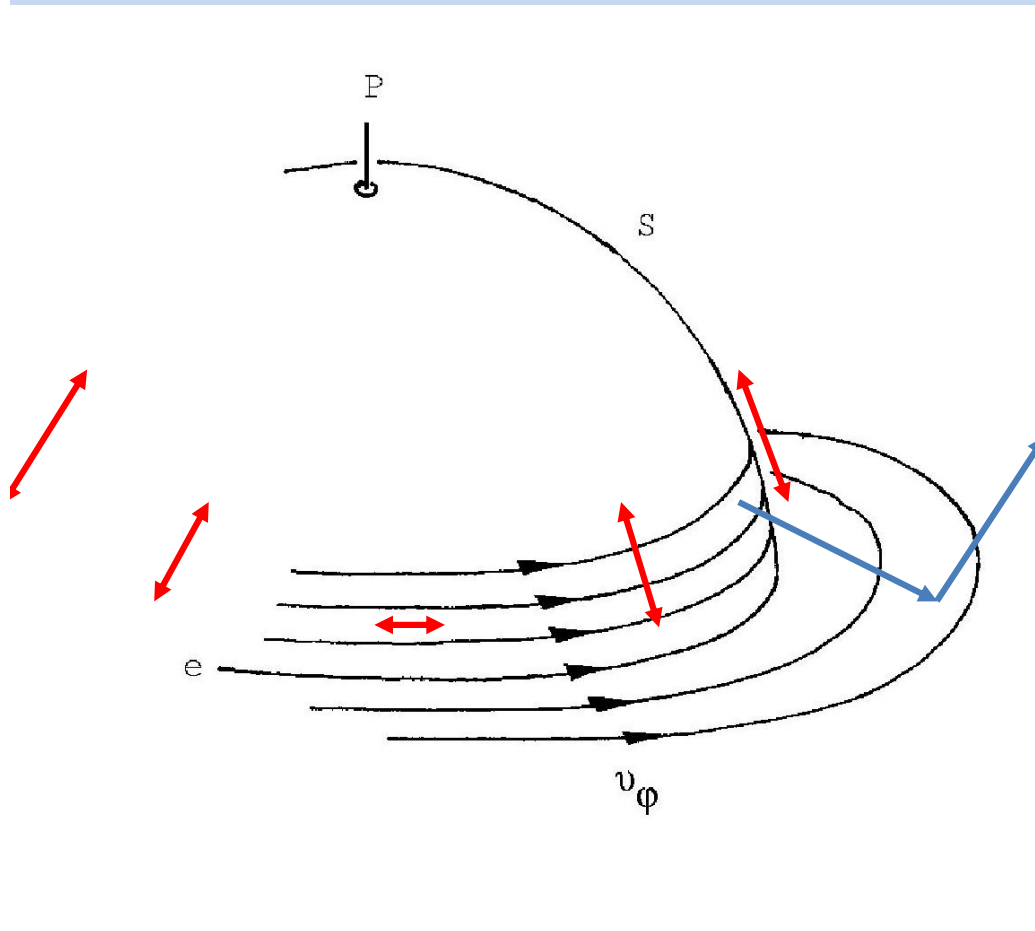


Figure 6. Contour plot of PD and PA in the 2–8 keV energy band obtained with *xspec*. The data have been fitted with two *polconst* models separately for the *diskbb* (pink colours) and *comptt* (green colours) components. *Left panel*: The PA of *diskbb* and *comptt* are left free. *Right panel*: The PA of *diskbb* was assumed to differ from the PA of *comptt* by 90° . Contour plots correspond to the 68.27%, 95.45% and 99.73% confidence levels, respectively.

Nonmagnetic NS: Cyg X-2



Where polarization can be produced?

Spreading layer (Inogamov & Sunyaev 1999) ?

Polarization from the half-sphere is small. The maximum is 0.18% at $i=60$ deg (Lapidus & Sunyaev 1985).

The narrow SL can produce higher polarization but likely below 1-2%.

Nonmagnetic NS: Cyg X-2

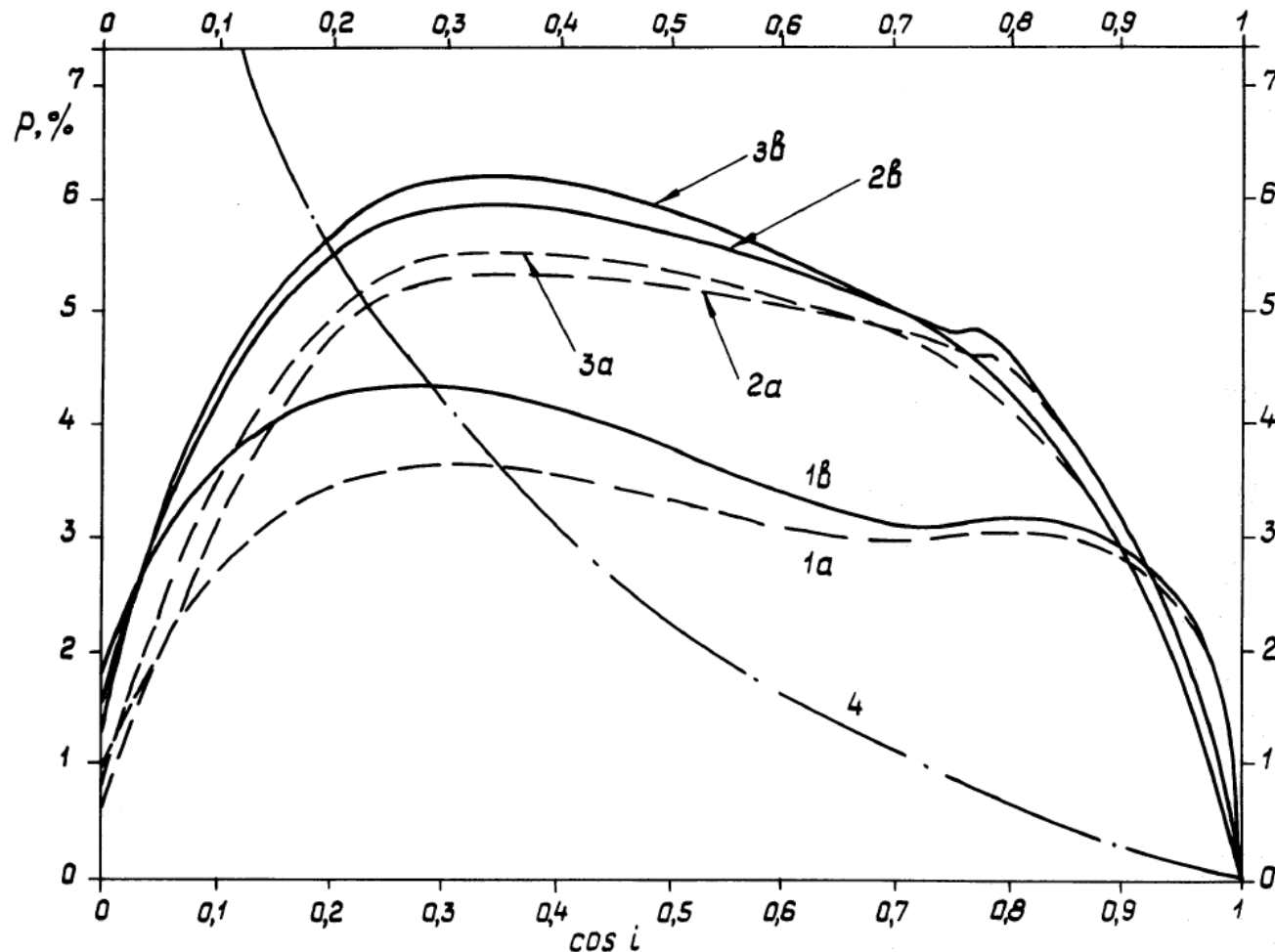


Figure 7. Degree of polarization of burster radiation between bursts. (1) $H/R_s=0.05$, (2) $H/R_s=0.1$, (3) $H/R_s=0.2$. Separately shown are (a) the polarization of disc radiation and (b) the polarization of radiation of the whole system 'disc+boundary layer'. The degree of polarization of radiation emitted by a semi-infinite electron scattering atmosphere (Chandrasekhar 1960) is also shown (4) for comparison.

Reflection from
 the accretion disk
 (Lapidus &
 Sunyaev 1985) ?

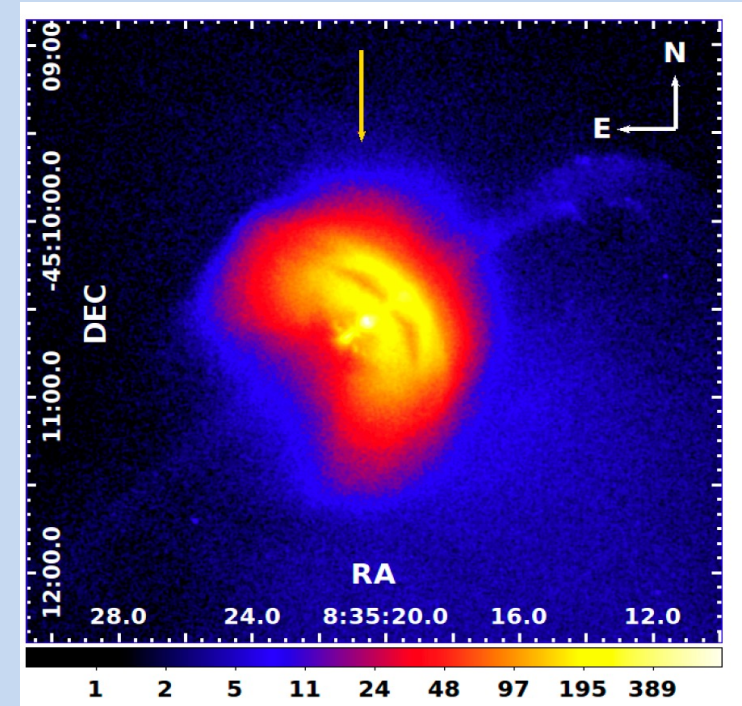
Up to 6% PD can
 be produced.

Models need to
 be updated to
 include relativistic
 effects.

Vela pulsar wind nebula

Vela PWN is powered by Vela pulsar

- Age: 11 ky
- Distance: 290 pc
- Rotation period: 89 ms
- Spin-down rate: 1.25×10^{-13} s/s
- Spin-down luminosity: 7×10^{36} erg s⁻¹
- Characteristic age: 11000 yr
- Transverse velocity: 65 km s⁻¹



Vela pulsar wind nebula

1. Vela pulsar
2. Inner arc
3. Outer arc
4. Inner jet
5. Counter jet
6. Shell
7. Outer jet

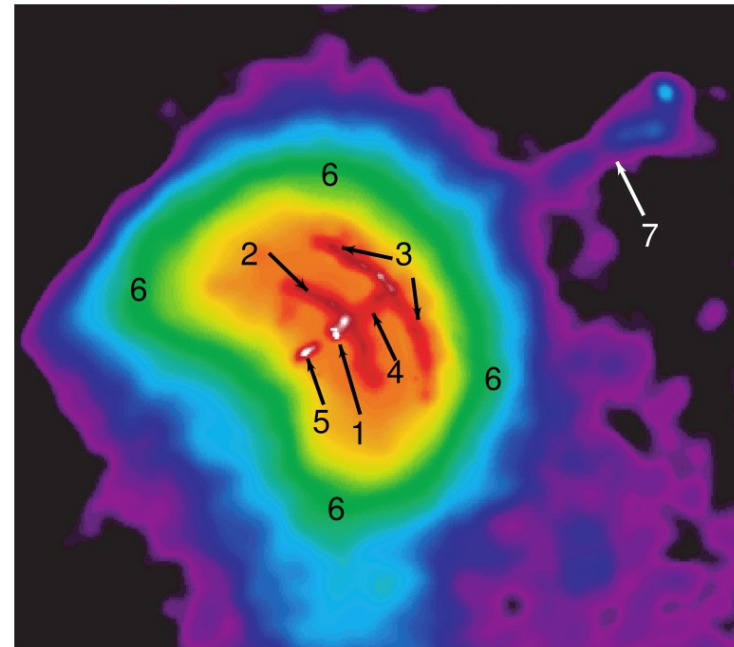
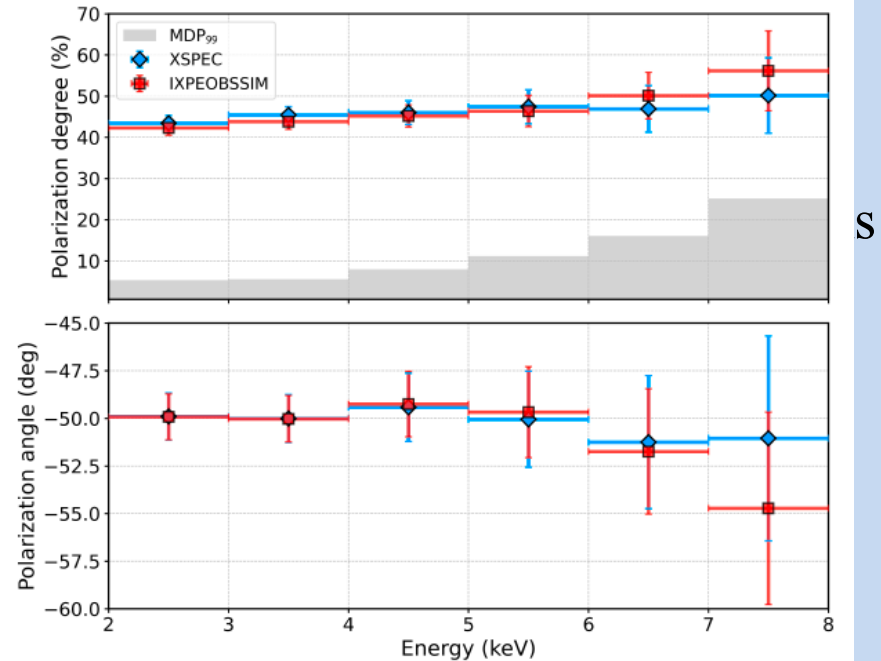
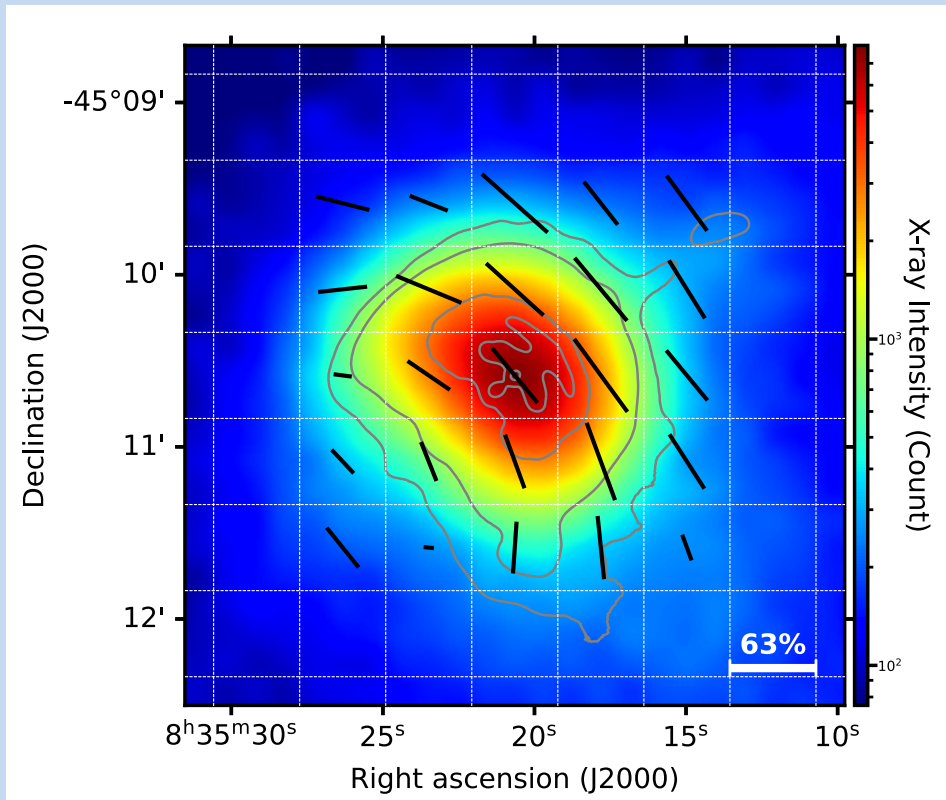


FIG. 2.—*Chandra* ACIS-S3 image, $2'1 \times 2'7$, of the Vela PWN showing the structural elements: (1) the Vela pulsar, (2) the inner arc, (3) the outer arc, (4) the inner jet, (5) the counter jet, (6) the shell, and (7) the outer jet.

Pavlov et al. 2003

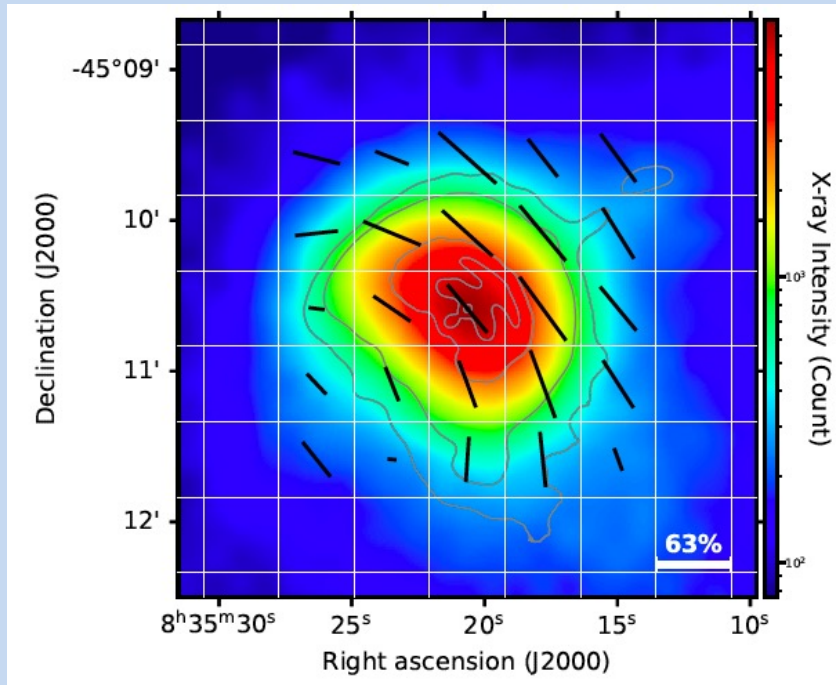
Vela PWN

IXPE observed Vela PWN for 860



- The magnetic field is **highly symmetric** about the pulsar jet axis.
- The curved and symmetric PA pattern implies **some loss of average polarization** in each bin.

Vela PWN

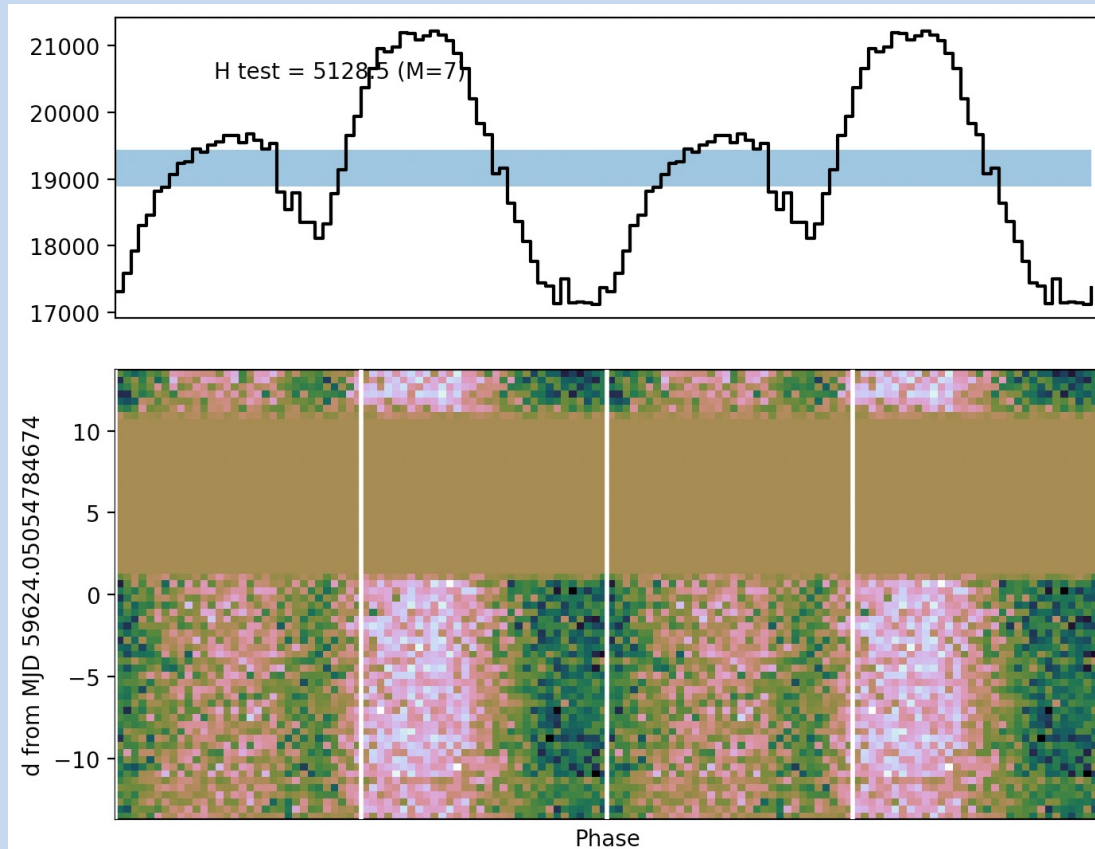


- 30''×30'' independent square regions
- Maximum PD = 63%
- the orientation of lines show PA at 90° to the EVPA
 - the direction of the projected magnetic field
- The magnetic field is **highly symmetric** about the pulsar jet axis.
- The curved and symmetric PA pattern implies **some loss of average polarization** in each bin.

This PD approaches the limit allowed by synchrotron theory and implies that, unlike SNR shocks, the PWN accelerates electrons with little or no turbulence, producing emission in a highly uniform magnetic field.

Magnetar 4U 0142+61

- Observed for 1 Ms: Jan 31 – Feb 14, Feb 25-27



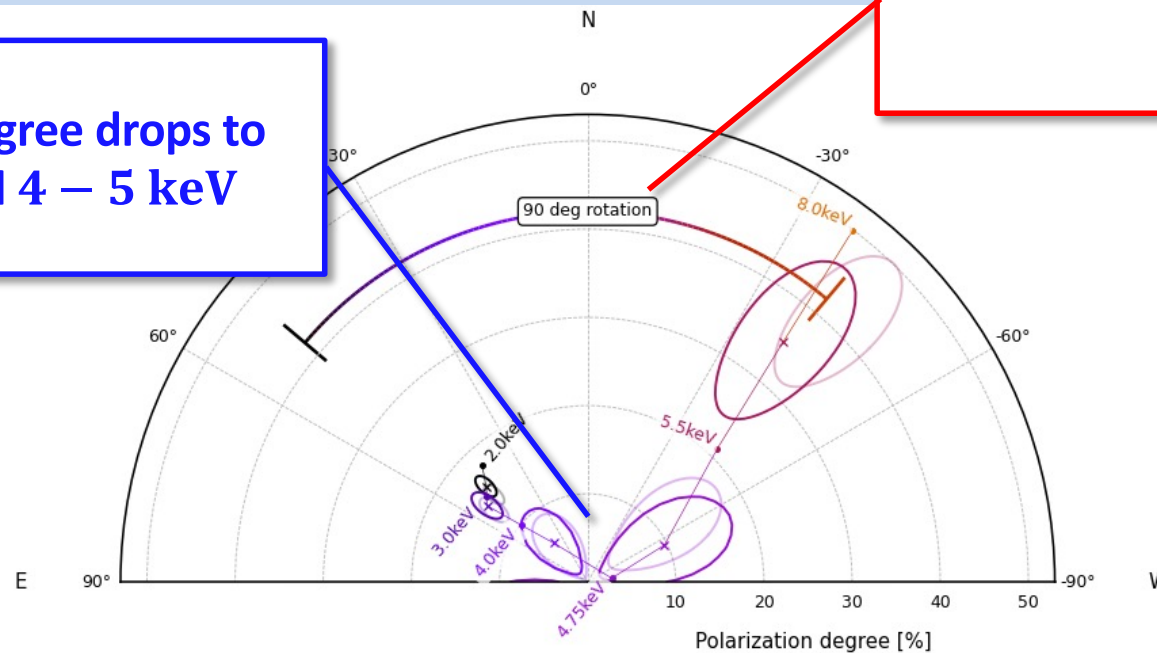
Measured value	
ν (s)	0.115079332(8)
$\dot{\nu}$ (Hz s ⁻¹)	-2.1(7) × 10 ⁻¹⁴
MJD 59624.051	

Magnetar 4U 0142+61

Phase-integrated/energy-dependent analysis

Polarization angle swings by 90°

Polarization degree drops to ~ 0 at around 4 – 5 keV



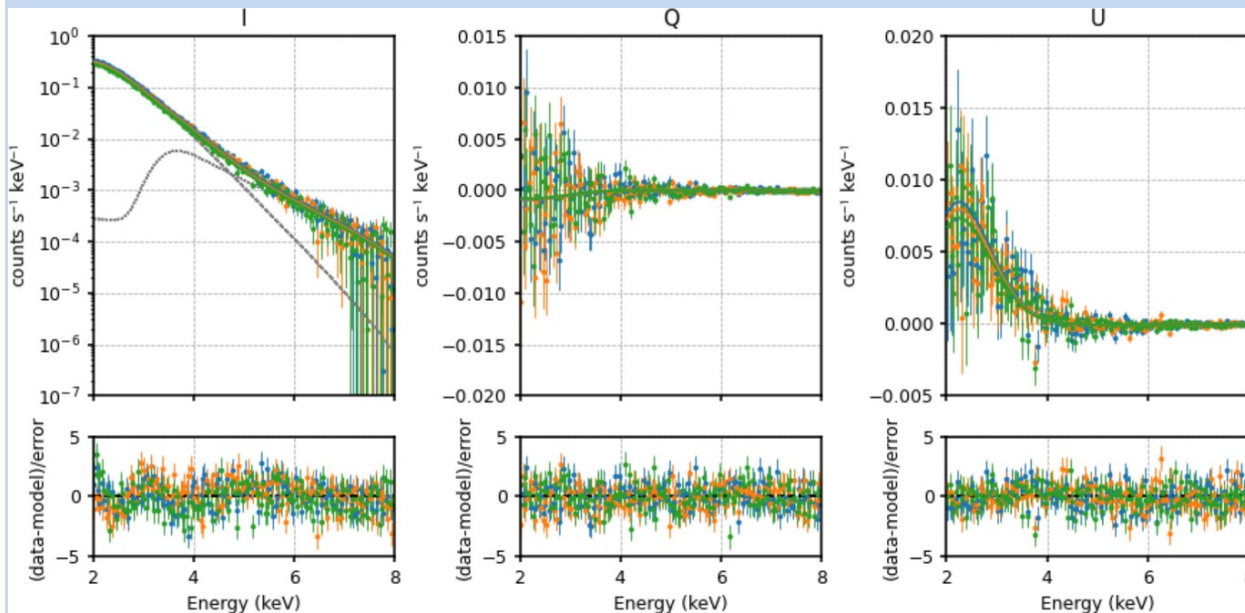
PCUBE	2-3 keV	3-4 keV	4-4.75 keV	4.75-5.5 keV	5.5-8 keV
PD (%)	14 ⁺¹ ₋₁	13 ⁺¹ ₋₁	5 ⁺³ ₋₃	11 ⁺⁵ ₋₅	41 ⁺⁷ ₋₇
PA (deg)	47 ⁺² ₋₂	52 ⁺³ ₋₃	36 ⁺¹⁷ ₋₁₇	-54 ⁺¹⁴ ₋₁₄	-44 ⁺⁵ ₋₅

Spectro-polarimetric analysis

Polarimetric analysis

Phase-integrated/energy-dependent analysis

- Two distinct components, e.g., blackbody + truncated power law
- Assume polarization is energy independent for each component

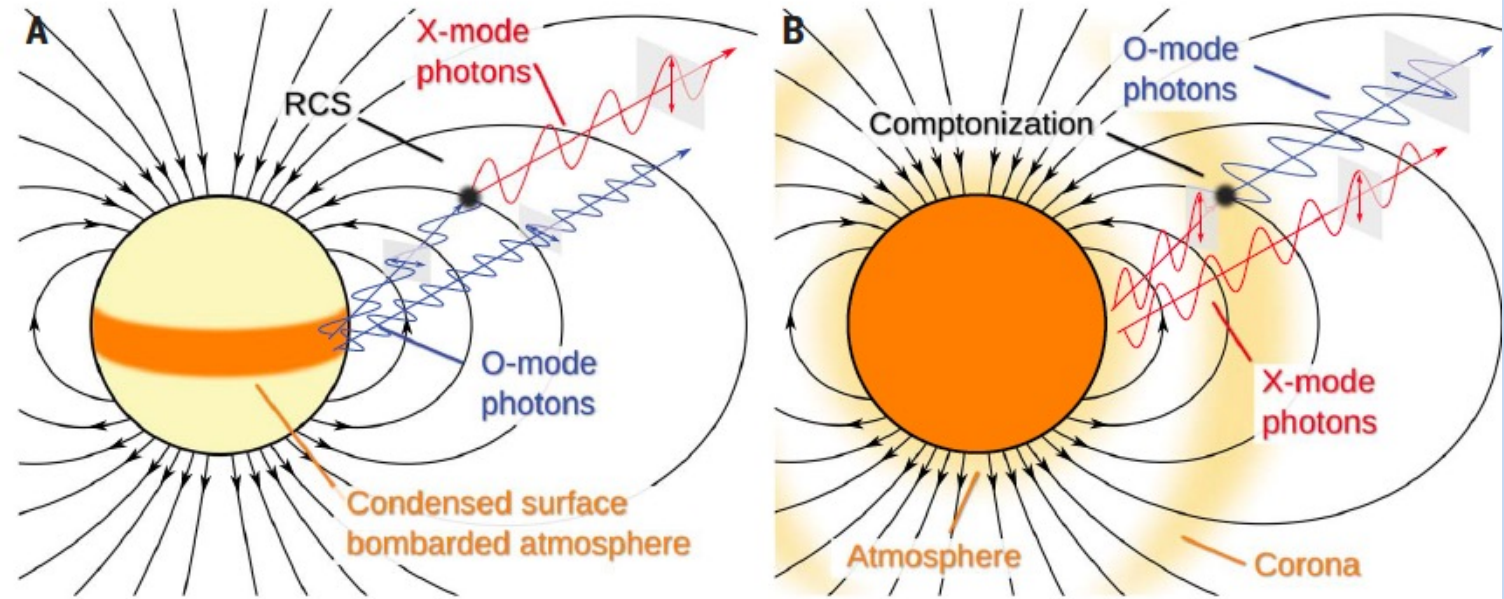


$$f * \text{TBABS} * (\text{BB} * \text{PC} + \text{TPL} * \text{PC})$$

Fit parameters	
n_H	0.57 (frozen)
kT	$0.448^{+0.001}_{-0.002}$
PD_{BB}	$0.168^{+0.008}_{-0.008}$
PA_{BB}	48^{+1}_{-1}
Γ	$2.67^{+0.04}_{-0.07}$
E_{trc}	$3.38^{+0.04}_{-0.02}$
PD_{PL}	$0.23^{+0.04}_{-0.04}$
PA_{PL}	-44^{+5}_{-5}

Theoretical interpretation

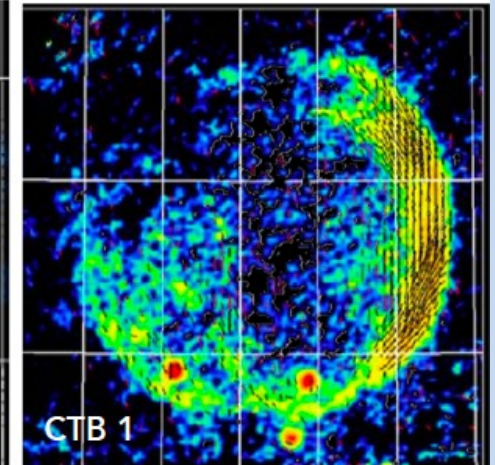
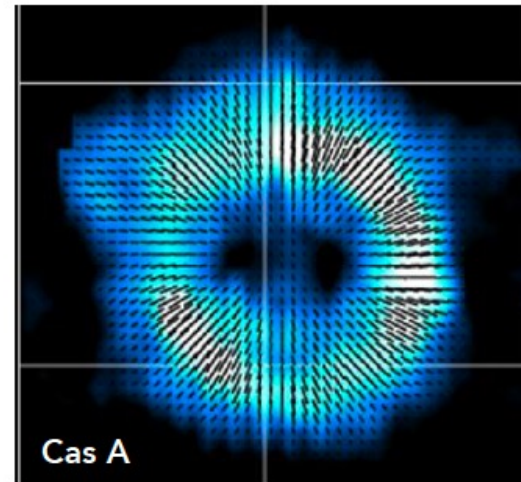
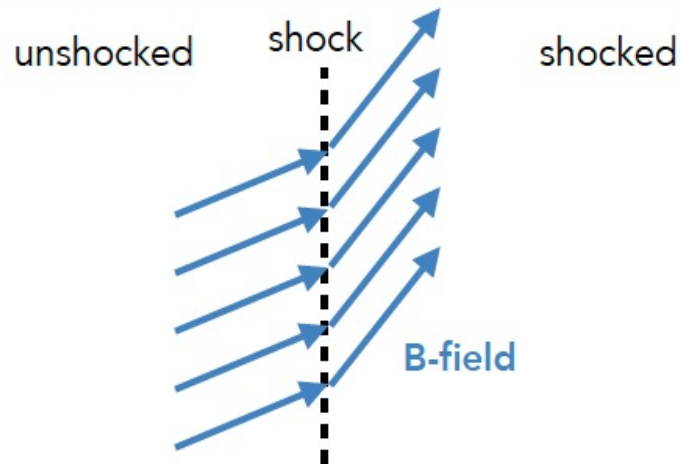
Fig. 4. Schematic illustration of the proposed theoretical scenarios. (A) Thermal radiation emitted by an equatorial belt on the condensed surface of the magnetar (or an atmosphere with an inverted temperature gradient), then reprocessed by RCS in the magnetosphere. **(B)** Radiation from the whole surface reprocessed by (unsaturated) thermal Compton scattering in a near-surface atmospheric layer, then additional (saturated) Compton scattering in an extended corona.



The dark orange areas on the NS surface indicate the emitting regions. Black lines with arrows indicate the (dipole) magnetic field lines. The gray rectangles along the photon trajectories highlight the polarization plane and the oscillating electric field.

Supernovae remnants

Radio polarization: the radial magnetic field puzzle

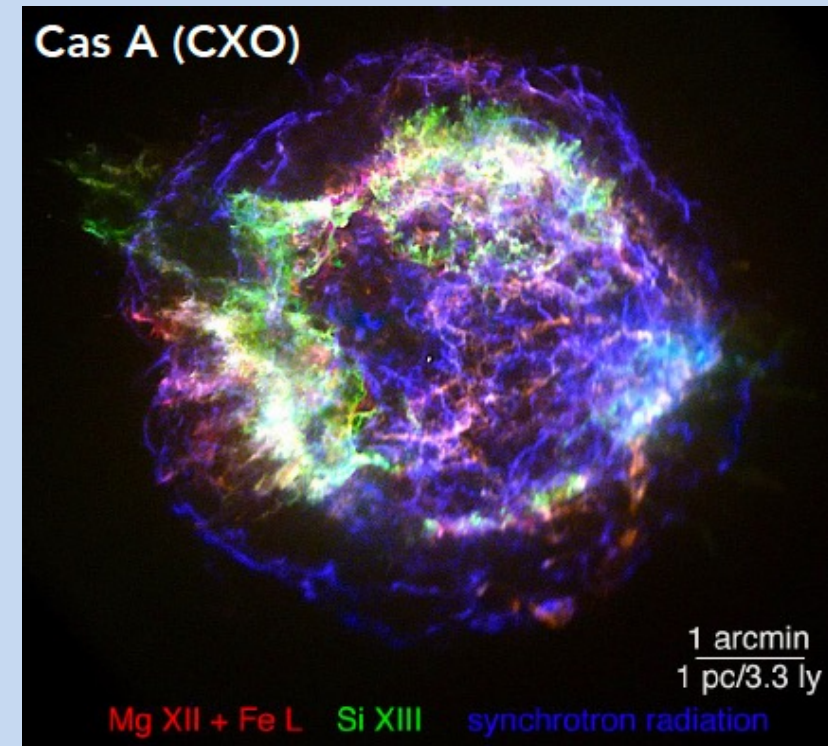


Dubner&Giacani (2015),
(Magnetic-field vectors)

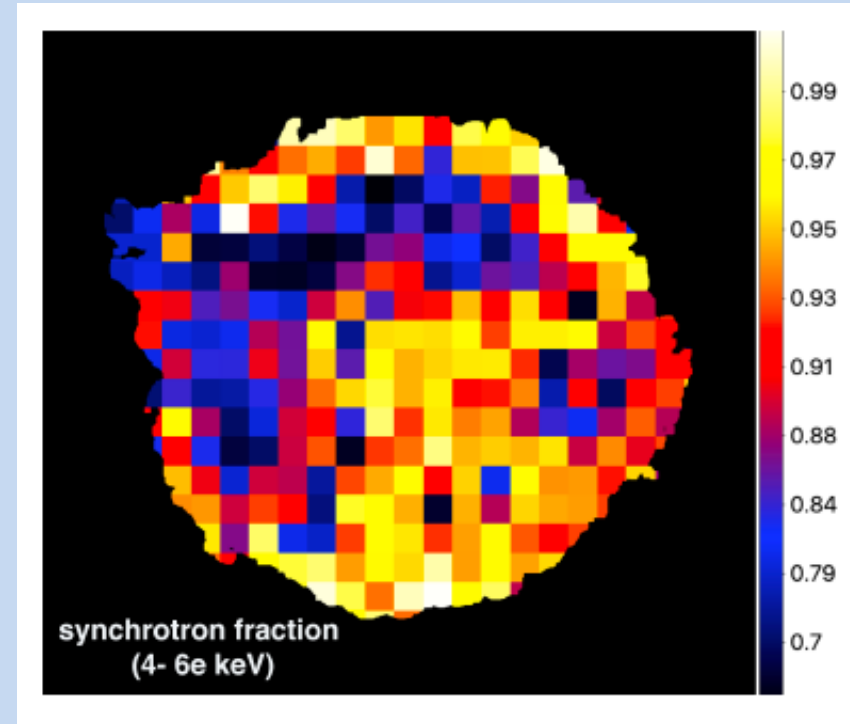
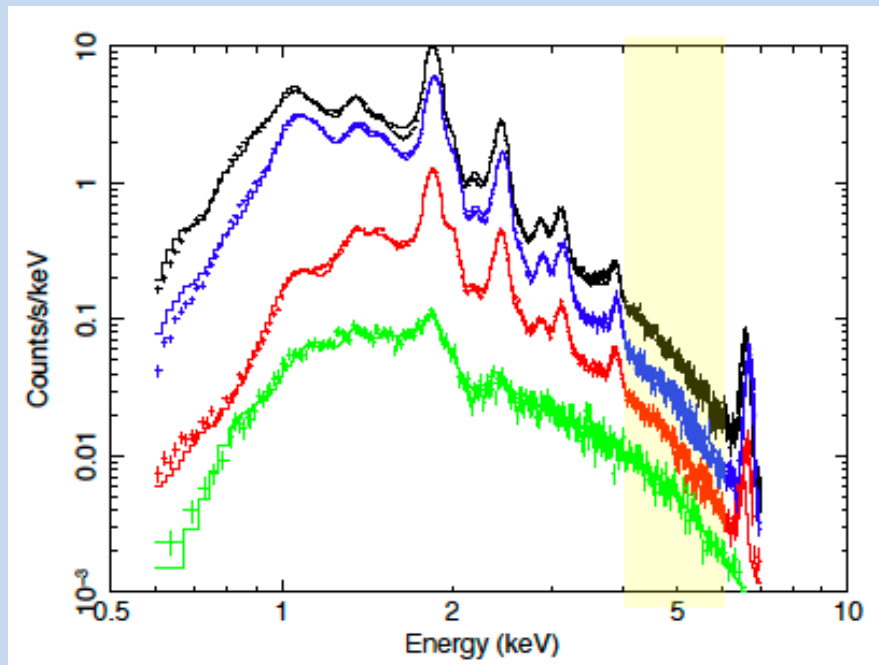
- Synchrotron radiation:
 - polarization vector perpendicular to magnetic direction
 - intrinsically polarized up to 70-80%
- Mature SNRs (≈ 2500 yr): tangentially oriented fields
 - Sensible: shock compresses tangential B-field components only
- Young SNRs (≈ 2500 yr): radially oriented B-fields and low pol. degree (Cas A: PD \sim 5%)
 - Poorly understood

X-ray synchrotron radiation from Cas A

- Cas A: ~350 yr old core-collapse SNR ($r=2.6$ pc)
- X-ray emission:
 - bright line emission
 - continuum dominated by synchrotron
- X-ray synchrotron radiation
 - ~10-100 TeV electrons
 - Fast radiative cooling: need fast acceleration
 - Requires *strong B-field turbulence* ($\delta B/B \sim 1$)
 - Only near shock front: X-ray synchrotron filaments are 1-2" thin $\rightarrow \lesssim 10^{17}$ cm, $B \approx 250 \mu\text{G}$
- Peculiar for Cas A: X-ray synchrotron emission from reverse (inner) shock



X-ray synchrotron radiation from Cas A



- Lines dominate the X-ray spectrum, but continuum dominates in 4-6 keV
- Chandra spectral modeling: 50—99% dominated by synchrotron
- Synchrotron component associated with forward shock & reverse shock in West

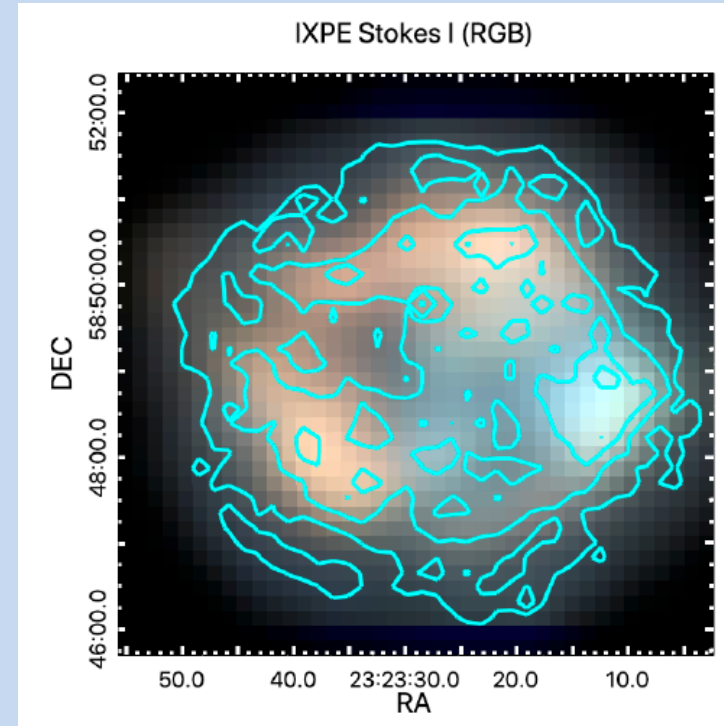


Goals of X-ray polarization measurements

- What is the polarization degree (PD)?
 - Could be higher than radio (>5%):
 - coming from smaller ($l \sim 10^{17}$ cm) regions
 - X-ray spectrum steeper than radio ($\Gamma_X = 3.2$ vs $\Gamma_R = 1.7$): higher intrinsic PD
 - Reasons for being lower than radio:
 - Near shocks: higher turbulence in B-field
- What is B-field orientation?
 - Tangential as imparted by shock compression
 - Random: due B-field randomization downstream (Bykov+ '20)?
 - Radial: like the radio, but now probe the $l \sim 10^{17}$ cm from shock fronts!

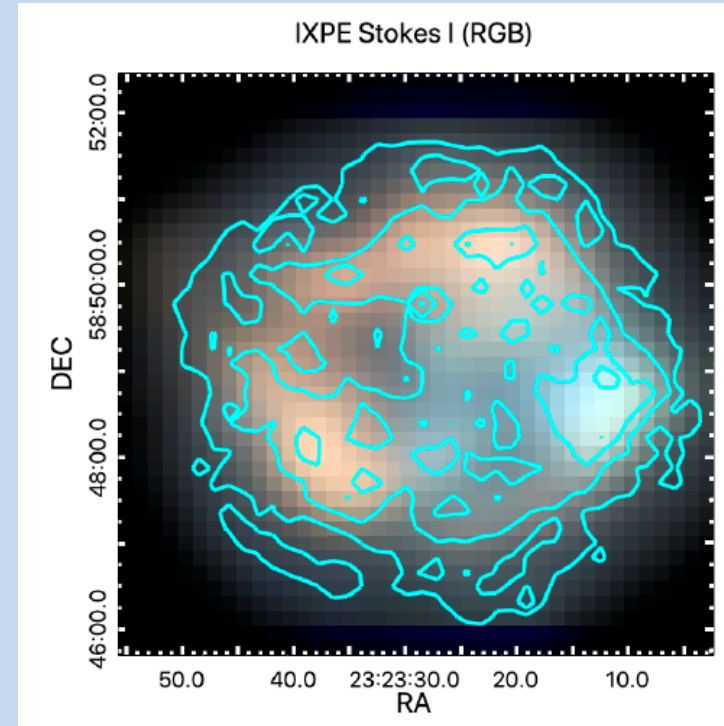
IXPE observations of Cas A

- Cas A: IXPE first science target!
- Observations: January 11-29, 2022 (~900 ks)
- Initially many calibration/SW issues:
 - bending boom on orbital phase
 - corrected in released event list
 - remaining spurious offsets (removed by team)
 - 2.5' remaining WCS error (corrected for by team)
 - uncertainties about correctness u and q columns PI/energy reconstruction imperfect (charge buildup) and det. unit dependent
- Effective exposure: 819 ks

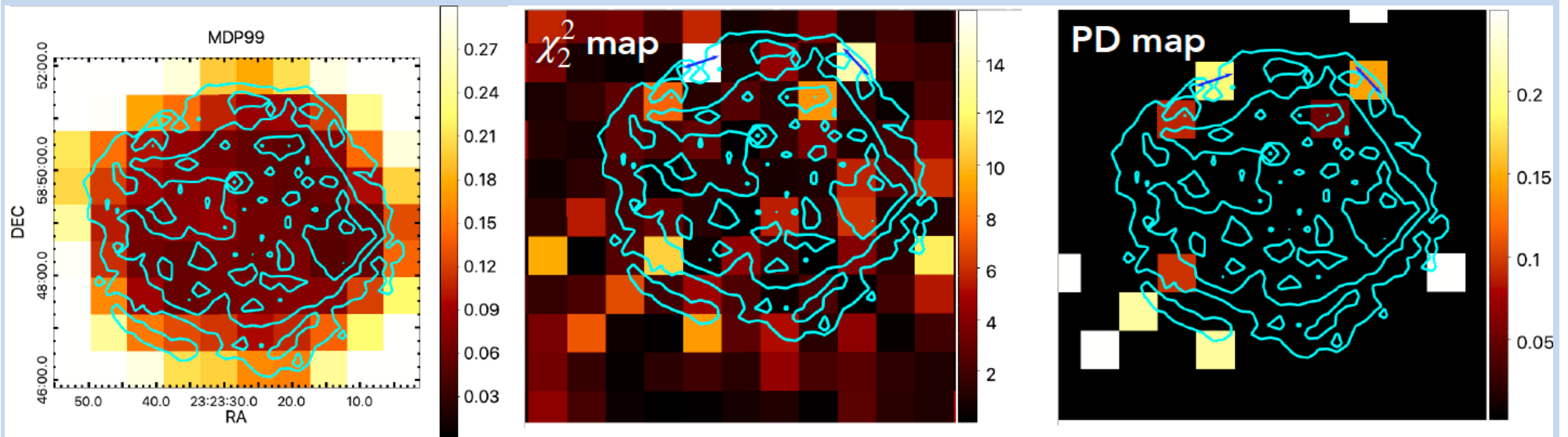


IXPE observations of Cas A

- Cas A: IXPE first science target!
- Observations: January 11-29, 2022 (~900 ks)
- Initially many calibration/SW issues:
 - bending boom on orbital phase
 - corrected in released event list
 - remaining spurious offsets (removed by team)
 - 2.5' remaining WCS error (corrected for by team)
 - uncertainties about correctness u and q columns PI/energy reconstruction imperfect (charge buildup) and det. unit dependent
- Effective exposure: 819 ks



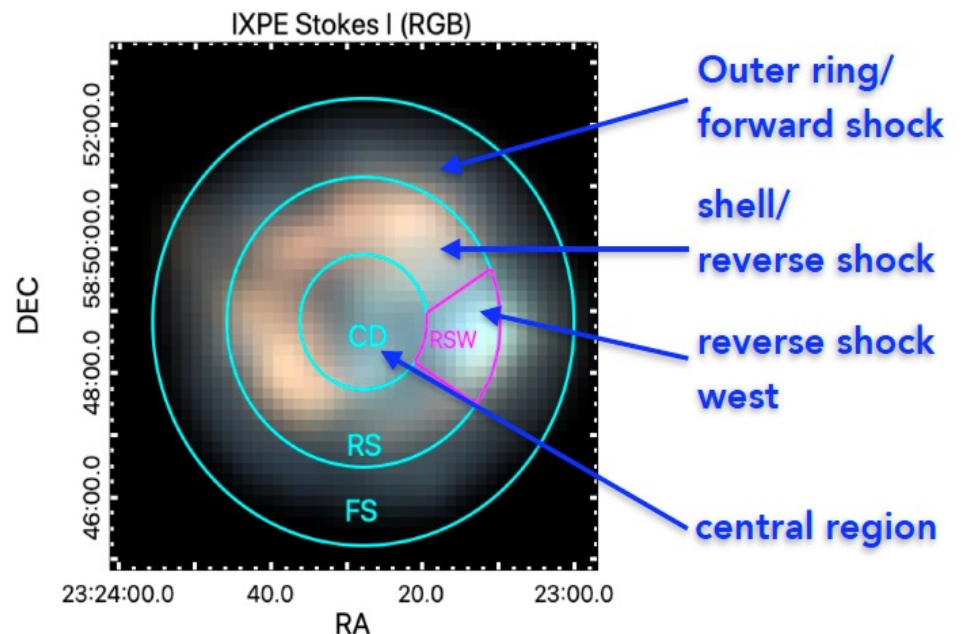
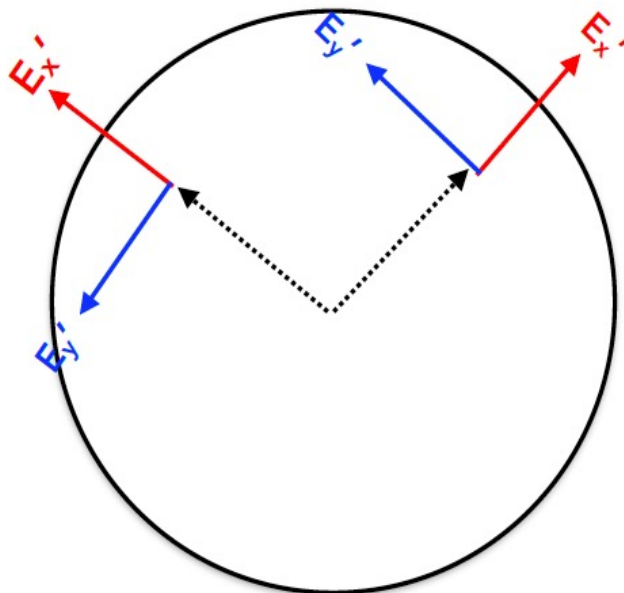
IXPE observations of Cas A



- MDP99 for Cas A (42" pixels): ~6—18% (3-6 keV)
- We searched for polarization signals using various pixel sizes (~26"—100")
- Typically two pixels at $>3\sigma$ ($\chi^2 > 11.8$) found, but position shifts for different binnings
- Cas A covered by ~200 resolution elements:
 - ~0.5 spurious signals at 3σ level expected → hints for polarization, no solid detections

IXPE observations of Cas A

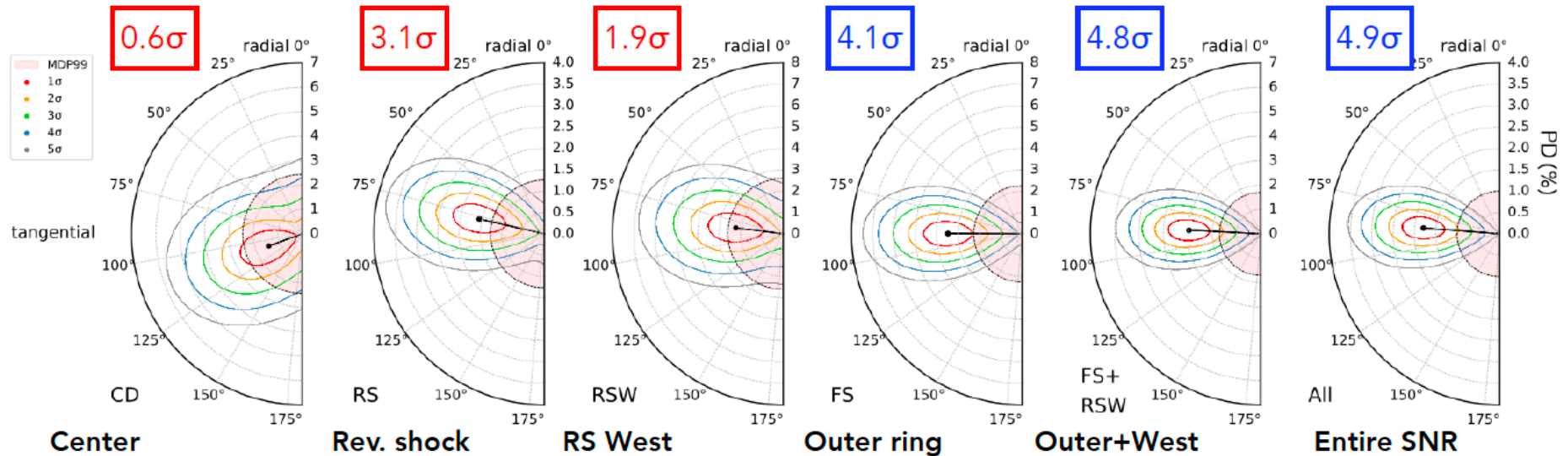
Analysis assuming circular symmetry



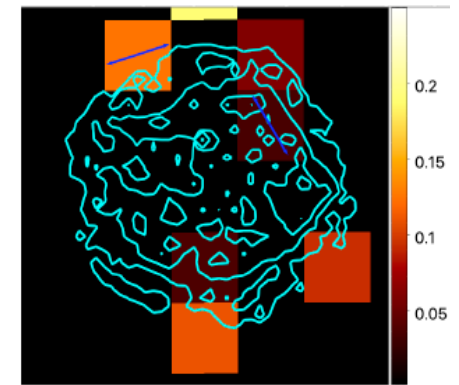
- No solid detections for pixel analysis: PD low, but how low?
- Expectations: either a radial magnetic field (radio) or tangential (shock compression)
- By sphericity of shell: circular symmetry expected anyway
- Method: for each location/per event specify local Stokes parameters Q' and U'
 - Can now sum q' and u' over very large regions: annuli

IXPE observations of Cas A

Results assuming circular symmetry

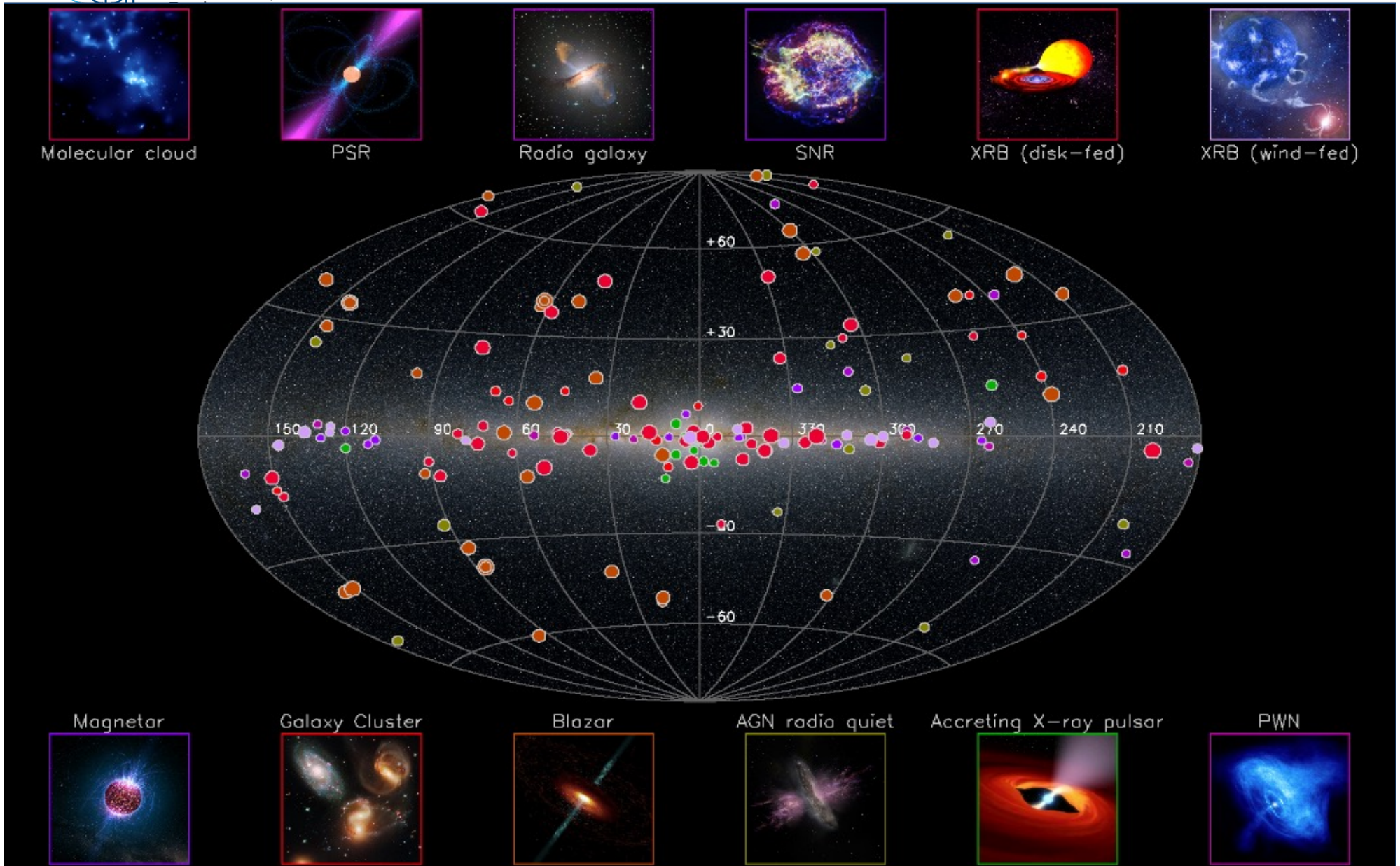


- For the outer shock region and FS+W and All we have now detections at the 4–5σ level!
- The polarization degree is low: 2—3.5%
 - After correction for thermal contamination: 2.4–5%
- The polarization vectors indicate a tangential direction: radial magnetic field!
 - Similar/lower PD than radio; same orientation
 - NB: X-rays confined to shocks, radio for whole shell



- X-ray polarization for Cas A is low and difficult to detect
 - Requires circular symmetry assumption to detect at $\sim 5\sigma$ level!
 - PD is 2–4.5% similar to radio
- By nature of X-ray synchrotron emission: polarization pertains to regions with 10^{17} cm of shock
- Polarization degree is equal or smaller than in the radio band
- Polarization vectors suggest radial magnetic field
 - Contrary to expectation at the shock front
 - Radial magnetic-field (bias?) present in X-ray synchrotron filaments with 10^{17} cm of shock
 - Constrains length scales for B-field reorientation

SKY MAP OF X-RAY POLARIZED SOURCES IN 2025?



Conclusions

IXPE has opened a new “X-ray polarimetry” window to the Universe.

Observations of X-ray polarization are already revolutionizing our understanding of magnetars, pulsars and pulsar-wind nebulae, SNR, accreting neutron stars and black holes, and blazar jets.